U.S. DEPARTMENT OF THE INTERIOR

U.S. GEOLOGICAL SURVEY

THE VENUS GEOLOGIC MAPPERS' HANDBOOK

SECOND EDITION

COMPILED BY KENNETH L. TANAKA[1]

WITH CONTRIBUTIONS FROM HENRY J. MOORE[2], GERALD G. SCHABER[1], MARY G. CHAPMAN[1], ELLEN R. STOFAN[3], DONALD B. CAMPBELL[4], PHILIP A. DAVIS[1], JOHN E. GUEST[5], GEORGE E. MCGILL[6], PATRICIA G. ROGERS[7], R. STEVEN SAUNDERS[3], AND JAMES R. ZIMBELMAN[8]

Open–File Report 94-438

Prepared for the National Aeronautics and Space Administration

This report is preliminary and has not been reviewed for conformity with U.S. Geological Survey editorial standards. Any use of trade, firm, or product names is for descriptive purposes only and does not imply endorsement by the U.S. Government.

[1]*U.S. Geological Survey, 2255 N. Gemini Dr., Flagstaff, AZ 86001*
[2]*U.S. Geological Survey, 345 Middlefield Rd., Menlo Park, CA 94025*
[3]*Jet Propulsion Laboratory, 4800 Oak Grove Dr., Pasadena, CA 91109*
[4]*Space Science Bldg., Cornell Univ., Ithaca, NY 14853*
[5]*Univ. of London Observatory, Mill Hill Park, London, NW72QS UK*
[6]*Dept. of Geology and Geography, Univ. of Massachusetts, Amherst, MA 01003*
[7]*NASA Headquarters, Code SL, 300 E Street, S.W., Washington, DC 20546*
[8]*Center for Earth and Planetary Science, National Air and Space Museum, MRC 315, Smithsonian Institution, Washington, DC 20560*

TABLE OF CONTENTS

INTRODUCTION

Radar images and other data acquired by the Magellan spacecraft make an exciting new venture possible: the geologic mapping of the planet Venus. Such mapping will form a basis for determining the planet's geologic history and understanding its geologic processes. The Venus Geologic Mapping (VMAP) program has been instituted to fulfill these goals and to conduct complete systematic scientific investigations of Venus. These complete studies will result in a set of published geologic quadrangle maps of all of Venus. VMAP is the most ambitious mapping program in terms of size and complexity yet attempted by planetary geologists. The VMAP program is made possible because of the complete coverage of Venus with radar images, altimetry, and data on physical-electrical properties.

The Magellan spacecraft was launched from Kennedy Space Center in Florida on 4 May 1989, entered orbit around Venus on August 10, 1990, and acquired the first radar images 6 days later. The radar is virtually unaffected by the thick Venusian atmosphere, and the radar images have a higher resolution (120-360 m) than has been achieved by Earth-based or other spacecraft missions. Magellan images, altimetry, and data on physical-electrical properties have revealed unparalleled details of mountain ranges, high plateaus, volcanoes, vast volcanic plains, lava flows, and areas of extensively deformed crust.

The map series consists of 62 quadrangles at 1:5,000,000 scale to be published in the Miscellaneous Investigations Map Series of the U.S. Geological Survey (USGS) (fig. 1). This VMAP program has been sponsored initially by NASA's Venus Data Analysis Program (VDAP), followed by NASA's Planetary Geology and Geophysics Program (PGG). These programs are administered by NASA Headquarters and coordinated by the USGS Branch of Astrogeology (Appendix A). Initial map proposals in 1992 were reviewed by the VDAP review panel; subsequent new proposals have been reviewed by the Lunar and Planetary Geoscience Review Panel. Mapping progress, workshop organization, and science issues are overseen by the VMAP Steering Group (Appendix A). USGS staff are responsible for base-map production and distribution, map editing, geographic name assignments, and geologic map production.

The basic products of the VMAP program are the 1:5,000,000-scale geologic maps of quadrangles, which will provide meaningful descriptions of the geology of the quadrangles and support various interpretive topical studies. Adherence to established mapping principles should preserve the value of the map despite the inevitable progress in geologic interpretation. Of course, such principles can be applied through various creative approaches. Geologic mapping is no mere mechanical exercise, because it requires interpretation of the distributions of backscatter and landforms portrayed by radar images as laterally continuous rock units formed by processes consistent with the image and other data; a geologic history, based on relative ages, is established using superposition and intersection relations among the rock units.

This handbook has been produced to guide geologic mappers in the VMAP program to meet the following challenges: (1) to gain an understanding of Magellan data and their bearing on the interpretation of geologic terrain, (2) to facilitate the application of conventional and special planetary mapping techniques to Venus, and (3) to promote continued usage of USGS guidelines for map publication. To first order, geologic mappers will employ standard photogeologic techniques on synthetic aperture radar (SAR) backscatter mosaics; refinements will result from analyses of high-resolution images, altimetry, and data on physical-electrical properties. Mappers will no doubt encounter specific mapping problems not addressed here that will require their own creativity and judgment to resolve (at times with assistance from others engaged in geologic studies of Venus).

In addition to this handbook, geologic mappers should refer to the guides to Magellan image interpretation by Ford and others (1989, 1993) and Michaels (1992), the special issues of *JGR–Planets*, "Magellan at Venus" (1992, v. 97, nos. E8 and E10), and "Suggestions to Authors of the Reports of the United States Geological Survey," edited by Hansen (1991). These publications will provide more complete and detailed technical information, illustrative figures, and style guidelines than are supplied in this handbook and will assist in understanding Magellan radar data and in producing geologic maps of Venus. Other relevant publications are offered in our "Recommended Reading" list.

We anticipate that mapping techniques and guidelines will evolve. We will appreciate suggestions for updates and additions to be included in future versions.

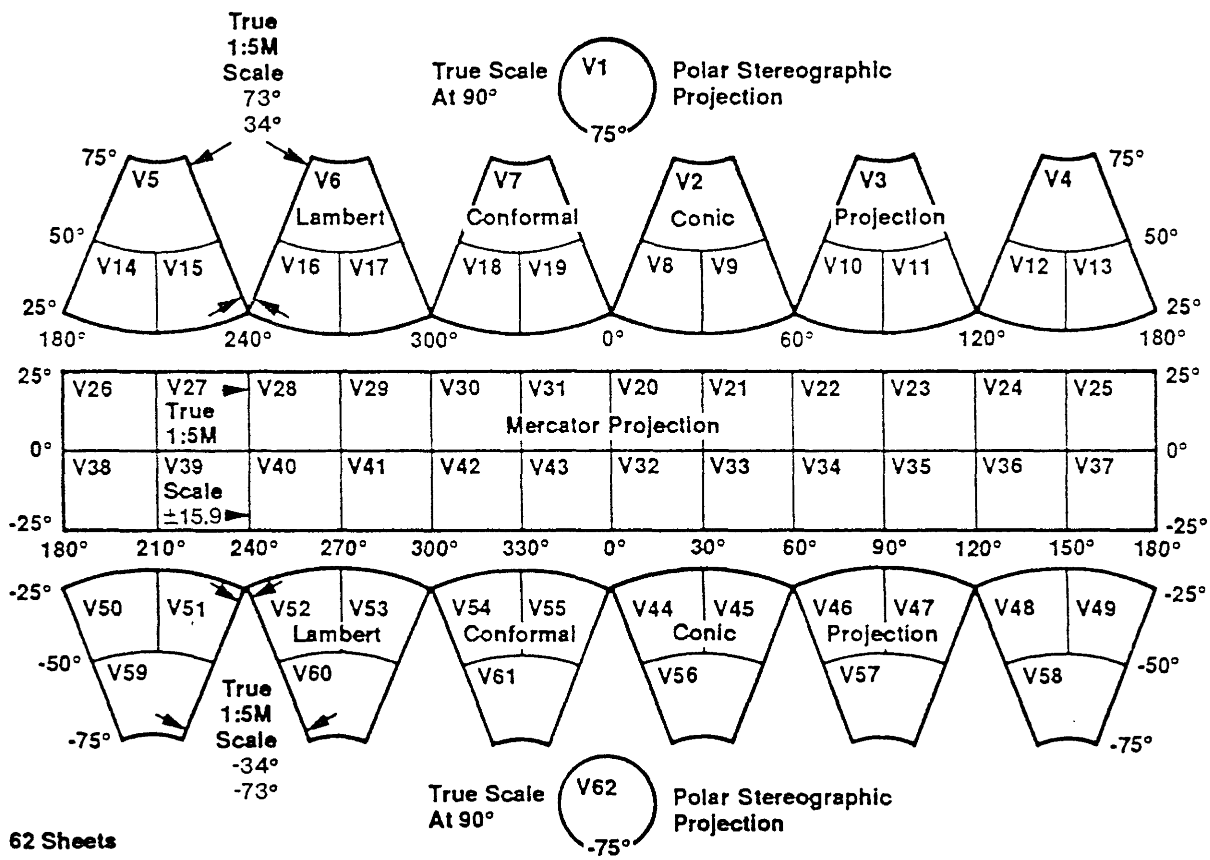

Figure 1. Index of 1:5,000,000-scale quadrangles of Venus.

OVERVIEW OF DATA SOURCES

Mission Summary

Magellan's global data on Venus have been acquired as part of a series of spacecraft investigations of the inner planets (Mercury, Venus, Earth, and Mars). The data are more complete than similar data for Earth (whose largely unmapped ocean floors make up 70 percent of its surface). The Magellan images, altimetry, and data on the physical-electrical properties of the surface of Venus were acquired at a wavelength of 12.6 cm and are very different from images and data acquired at optical wavelengths that have been employed for planetary geologic mapping and studies. The properties of surfaces that influence reflection of radio waves are not the same as those that influence the reflection at optical wavelengths. This factor must be considered when interpreting synthetic aperture radar (SAR) images and surface properties measured at radio wavelengths and when preparing geologic maps.

In this section we briefly discuss (1) the Magellan mission, (2) the radar instruments, (3) data acquisition and processing, and (4) data products that are or will become available. For detailed information, please see the Recommended Reading.

The Magellan radar mapping mission to Venus has provided SAR images of 98.3% of the planet's surface, as well as data on topography, small-scale surface roughness, radar reflectivity, and thermal emissivity—all of which cover similar percentages of the surface (Saunders and others, 1992). The images and the ancillary data are the resource materials for the VMAP program.

The Magellan spacecraft went into orbit around Venus with an orbit period of 3 hr. 25 min. and inclination of 85°. This corresponds to about 7.5 orbits per day and a total of 1,790 orbits during one 243-day rotation period (a 'cycle' in Magellan parlance). Periapsis of the orbit was at lat 9.9° N. and the motion of the spacecraft was from north to south during data acquisition. The altitude of the spacecraft was 294 km at periapsis and 2,100 km over the north pole. The 85° inclination angle for the orbit was chosen to allow imaging of the polar regions.

After orbit insertion, the first four weeks of the mission were devoted to engineering tests, but some test images were acquired as well. Systematic data collection began on 15 September 1990. Coverage was completed in cycle 1 on 15 May 1991, and in cycle 2 on 14 January 1992. Cycle 3, the last cycle in which systematic SAR data were obtained, ended on 14 September 1992. Cycle 4 mission operations focused on the collection of gravity data. Continuation of the Magellan mission beyond cycle 4 involved aerobraking to a low-altitude (250 km) circular orbit, acquiring high-resolution gravity data, and special experimenting.

Images of 83.7% of the planet's surface were obtained during cycle 1 with the SAR antenna looking to the east of the orbit plane (left-looking) (see Michaels, 1992, fig. 2); 54.5% was covered during cycle 2 with right-looking images and some left-looking images (Michaels, 1992, fig. 3); and 22.8% was covered during cycle 3 with left-looking images (chiefly for stereometric use with cycle 1 images). Coverage of

Venus with SAR images is summarized in Ford and others (1993; figs. 2.2, 2.4, 2.5, and 2.6).

The Magellan Radar Sensor

Many geologists are familiar with the techniques of photogeologic mapping and have a working knowledge of standard aerial photography, satellite images, and stereoscopy. Magellan SAR images are basically similar to photographs and images acquired in the visible wavelengths in that they faithfully portray landforms and topography. However, there are important differences between the SAR images and images acquired at visible wavelengths because of the source of illumination, the manner in which the radar echoes are translated into map distances, and the large wavelength of the radar. The surface is illuminated by the Sun for aerial photography and satellite imagery, whereas the SAR provides its own illumination. Geometric distortions or relief displacements in aerial photographs and satellite images are radial to the nadir, whereas those in SAR images are in the direction of the radar antenna. The large wavelength (12.6 cm) of the Magellan SAR results in scattering properties of the surface that are much different than those at visual wavelengths; these scattering properties vary with several parameters such as wavelength, polarization, and incidence angle of the transmitted radar waves and the fine- to coarse-scale roughness and physical-electrical properties of the surface. Thus, geologic mappers will need to be familiar with the characteristics of the Magellan radar system, how the data were acquired and processed, and responses of natural surfaces to incident radar energy so that they can intelligently analyze the data.

The Magellan spacecraft carries a single scientific instrument–a multi-mode radar sensor that operates in burst cycles. Each burst cycle consists of sequential synthetic aperture radar (SAR), altimetry, and radiometry measurements (Saunders and others, 1990, fig. 2; Saunders and Pettengill, 1991; Ford and Pettengill, 1992; Michaels, 1992, table 1 and fig. 1). The SAR and altimeter are active sensors that transmit radar waves and measure the radar echoes from the surface (backscatter or reflectivity) in oblique and vertical (near-nadir) viewing geometries, respectively (Pettengill and others, 1991). The radiometer passively measures the thermal emission from the surface at 12.6-cm wavelength by sampling the SAR receiver between radar echoes. The SAR and the radiometer operate through a narrow bandwidth, high-gain antenna (HGA), while the altimeter uses a separate, smaller horn antenna (ALTA) positioned to the side of the HGA. Magellan's SAR operates at angles of incidence between about 17° and 45.7° from the local surface normal. Incidence angles are smallest toward the poles and largest at periapsis (Pettengill and others, 1991; Saunders and others, 1992; Tyler and others, 1992). During each orbit the SAR imaged a strip about 20 km wide and 17,000 km long, alternately from the north pole to 57° S (intermediate swaths) and from 70° N to 70° S (delayed swaths). The three Magellan radar modes are briefly discussed below.

Synthetic aperture radar (SAR). Synthetic aperture radar (fig. 2) is a method of acquiring images of a surface (Tyler and others, 1992). Illumination of the surface is provided by transmitting radar energy to the surface through the SAR antenna and receiving the echoes or backscattered energies with the same antenna. Echoes are associated with specific areas on the surface (resolution cells) because of the known topography, spacecraft orbital parameters, large incidence angles, and motion of the spacecraft. This situation allows separation of echoes by time delay or range and by Doppler shift or azimuth (fig. 2). The range direction is called cross-track and the azimuth direction is called along-track.

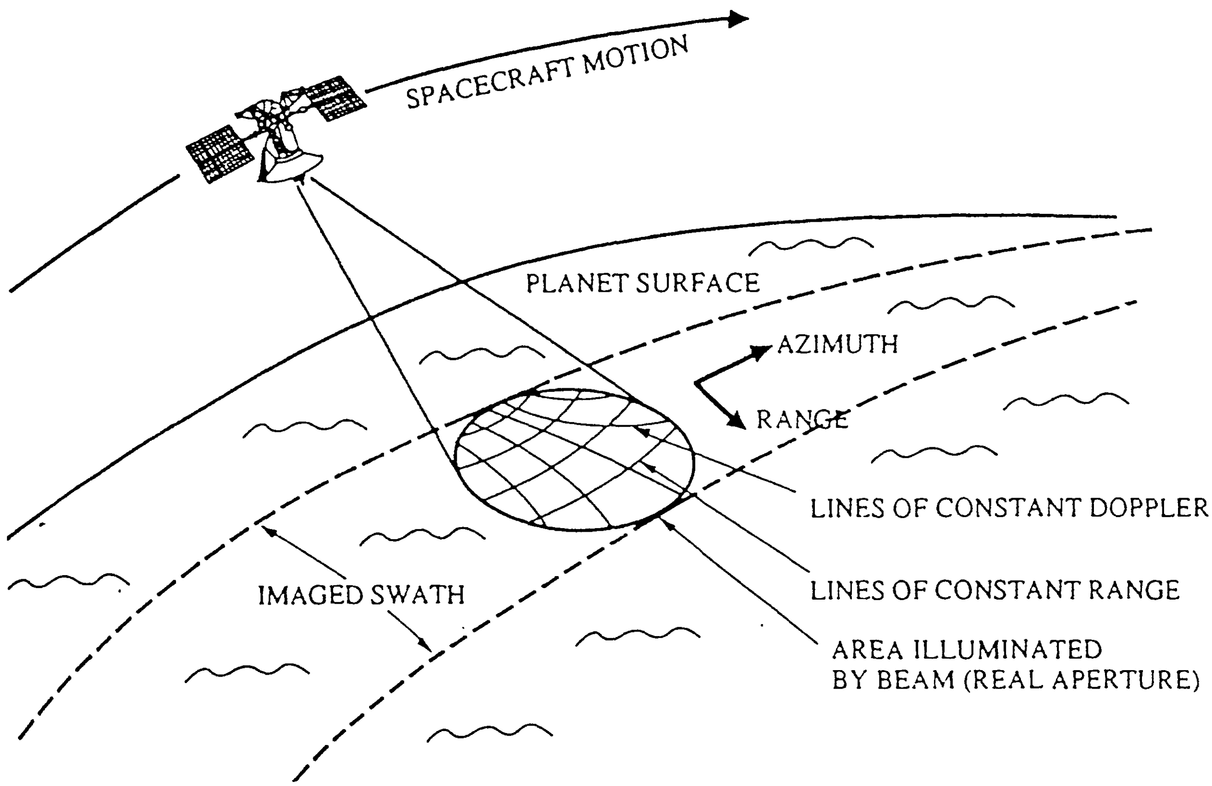

Figure 2. Method of data acquisition by the Magellan synthetic aperture radar (SAR) system; see text for discussion. (Reprinted from *Engineering & Science,* Spring 1991, v. LIV, no. 3, p. 16)

Several parameters control Magellan SAR image quality. The most important are spatial resolution, the number of "looks," amplitude resolution, signal-to-noise ratio, and incidence angle. The SAR was designed to produce a 120-m along-track or azimuth resolution. Cross-track or range resolution is governed by normal techniques of pulse encoding common to most radars and is a function of radar bandwidth and incidence angle. Range resolution varies from about 120 m near periapsis to about 280 m near the poles (Michaels, 1992, figs. 16, 17). These two resolution dimensions constitute a resolution cell. The backscattered echoes were resampled at a pixel spacing of 75 m for the construction of images. Each measurement of the power backscattered from a resolution cell is a single estimate of a random variable whose mean is the backscatter radar cross section. For Magellan, the number of looks (N) ranged from 5 near the equator to 15 near the poles (Saunders and others, 1992, table 3). If these estimates or looks are averaged to obtain a mean, then the standard deviation of this measurement of the mean is equal to the mean divided by $N^{1/2}$. The angle between the incident radar waves and the surface normal was varied to maintain an acceptable ratio of signal-to-noise as the altitude of the spacecraft above the surface varied. Decreasing the angle of incidence increases the returned power because of Venus' scattering law at 12.6-cm wavelength, and thus the decreased angle compensates for the increased signal loss as the distance to the surface increases (Pettengill and others, 1991).

Image pixel values (DN) are normalized backscatter cross sections and equal to the ratio of the measured mean backscatter cross section to the value predicted by the Magellan project scattering law (Saunders and others, 1992). Predicted values closely match empirically derived average backscatter behavior of the surface of Venus as a function of incidence angle (Muhleman, 1964). The pixel (DN) values range between 1 and 251, and each increment of 1 DN corresponds to an increment of 0.2 decibels (dB). Relative accuracy of the radar cross section is less than ±1 dB in the cross-track direction and ±2 decibels (dB) in the along-track direction. Performance checks during the mission verified that the radar sensor was operating according to sensitivity specifications.

The backscatter coefficient (also called backscatter cross section, sigma-zero, or σ_o) is a measure of the power of an echo from the surface. Because backscatter coefficients are of interest to mappers (as discussed later), a procedure for calculating them is given here. Normalized backscatter cross sections (σ_n) are ratios of backscatter coefficients to the expected backscatter cross section ($\sigma_v(\Theta)$) for a horizontal, level surface at the incidence angle (Θ) of the Magellan SAR image:

$$\sigma_n = \sigma_o/\sigma_v(\Theta).$$

Normaized backscatter cross sections (σ_n) are related to DN values by:

$$\sigma_n = 10^X,$$

where $x = 0.1[(DN - 1)/5 - 20]$. The normalizing equation used by the Magellan project for the expected backscatter cross section is given by:

$$\sigma_v(\Theta) = [0.118 \cos(\Theta+0.5)] [\sin(\Theta+0.5) + 0.111 \cos(\Theta+0.5)]^{-3}.$$

Sigma-zero (σ_o) is the product of σ_n and $\sigma_v(\Theta)$ (i.e., $\sigma_o = \sigma_n \times \sigma_v(\Theta)$) and $10 \log_{10} (\sigma_o)$ gives the value of σ_o in decibels.

The key parameters of Magellan's radar imaging system, as well as those for previously acquired radar data, are given in Table 1 of Michaels (1992).

Altimeter. The altimeter on Magellan measures the round-trip time of the transmitted signal and its echo (and therefore, the distance) between the spacecraft and the surface (Pettengill and others, 1991). Because of the orbital altitude and the need to improve the signal strength, the Magellan radar altimeter was designed to transmit 17 pulses and then to "listen" for their echoes. The pulses were transmitted and their echoes received through the altimeter horn antenna, which was pointed down toward the nadir. The strongest echoes usually come from smooth, level surfaces at the nadir, but in rough regions the echoes can be contaminated with echoes from nearby areas. The altimeter "footprint" is large (8 x 11 km at periapsis to 20 x 29 km near the poles), and several techniques are used to determine the spacecraft-to-surface distance. The altimetry data are combined with information on the spacecraft position relative to the planet's center of mass to produce a topographic map, which shows elevations in terms of planetary radii (Ford and Pettengill, 1992).

Shapes of the time-dispersed and (or) frequency-dispersed echoes and their amplitudes for each transmitted pulse from the altimeter horn antenna are dependent on the surface roughness at both wavelength and larger scales and on the surface reflectivities of the areas within the altimeter footprint. The shapes of the echoes (that is, the amplitudes as a function of time or frequency) are measures of the meter-scale surface roughness within the antenna footprint and can be fitted to several theoretical scattering functions (the scattering laws); delays or frequencies correspond to incidence angles from zero to about 10° or 30° (Tyler and others, 1992). The integrated power in the echoes provides an estimate of the backscatter cross sections at normal incidence.

Radiometer. The Magellan SAR antenna is used to estimate the brightness temperature of the surface in a passive mode. The procedures for making these estimates are beyond the scope of this handbook, but they are discussed by Pettengill and others (1992), who also list footprint dimensions. The estimated brightness temperatures at 12.6-cm wavelength are then compared with the black-body or physical temperatures of the surface. Physical temperatures of the surface are known from previous experiments (Pettengill and others, 1992).

Analysis of Magellan Radar Data

SAR images. SAR images are similar to aerial photographs and images acquired at visual wavelengths, because all three portray the morphology and moderate- to coarse-scale topography of the surface and its landforms. Morphology and topography are evident in SAR images because of the modulation of echo strengths by slopes. Echo strengths tend to increase with decreasing incidence angle. Thus, echoes from slopes facing the radar antenna are stronger and appear brighter in the images than those facing away from the radar antenna, but the magnitudes of the echo modulations also vary with surface properties. Some landforms with little or no relief, such as lava flows, can be recognized by patterns of backscatter that differ from those of the adjacent surfaces.

Magellan SAR echoes are thought to result primarily from two scattering mechanisms: quasi-specular and diffuse. Quasi-specular echoes are produced by mirrorlike reflections from facets oriented perpendicular to the SAR antenna

(Hagfors, 1964; Tyler and others, 1991) that are much larger than the wavelength of the radar (12.6 cm). Quasi-specular scattering dominates echoes at small incidence angles, but echo strengths decrease rapidly with increasing incidence angle and become weak to nonexistent relative to the diffuse echo at incidence angles near 10° to 30° or so (depending on the root-mean-square slope). Quasi-specular echoes are rare in Magellan SAR images because of the large incidence angles. Diffuse scattering is produced by wavelength-size roughness elements at and near the surface, which scatter the incident radar energy in all directions so that diffuse echoes are received at all incidence angles. Diffuse scattering dominates echoes at large incidence angles that are typically greater than ~30°, and the echoes also tend to become weaker with increasing incidence angle. However, this tendency is a function of the attributes of the wavelength-size scatterers on the surface (such as concentration, size-probability distribution, and dielectric properties). Diffuse echoes dominate the Magellan SAR images because of the large incidence angles.

Other applications and aspects of SAR data are discussed in the following numbered sections. This discussion highlights the derivation of several parameters and measurements and their relevance to geologic mapping, as well as important topographic effects, so that the mapper can make fullest use of the data.

1. *Backscatter coefficient.* The backscatter coefficient, as noted previously, is a measure of the power of an echo from the surface. The backscatter coefficient is a function of incidence angle, Θ, of the transmitted radar energy with the surface and the physical-electrical properties of the surface materials. Backscatter coefficients of planar level surfaces tend to be larger at small incidence angles than at larger incidence angles; similarly, surfaces tilted toward the radar tend to have large backscatter coefficients than surfaces tilted away from the radar. Concentrations of wavelength-size roughness elements at and near the surface also affect the backscatter coefficient. Roughness elements include rocks, surfaces of aa lava flows, near-surface voids, and other wavelength-size discontinuities. Large concentrations of roughness elements produce larger coefficients than smaller concentrations. Magellan SAR images contain quantitative information on backscatter coefficients because the DN values, as noted previously, are normalized by values of backscatter (Saunders and others, 1992). Of importance to the mapper is the information that can be gained about the properties of geologic map units. Some terrestrial data illustrating this application are given in figure 3; the literature should be consulted for further possibilities.

2. *Identification resolution.* The identification resolution of a SAR image is larger than the resolution stated in terms of pixel or cell size (120 m x 120 to 280 m) and is a function of landform shape, size, and backscatter properties and SAR incidence angles. Analyses of lunar radar images suggest that an observer begins to identify crater landforms when they are about four times the cell size of the radar (Moore and Thompson, 1988). Experience with spacecraft images at visual wavelengths yields similar results (Dial and Schaber, 1981). For Magellan SAR images, geologic mappers will learn by experience the sizes of landforms that they can identify.

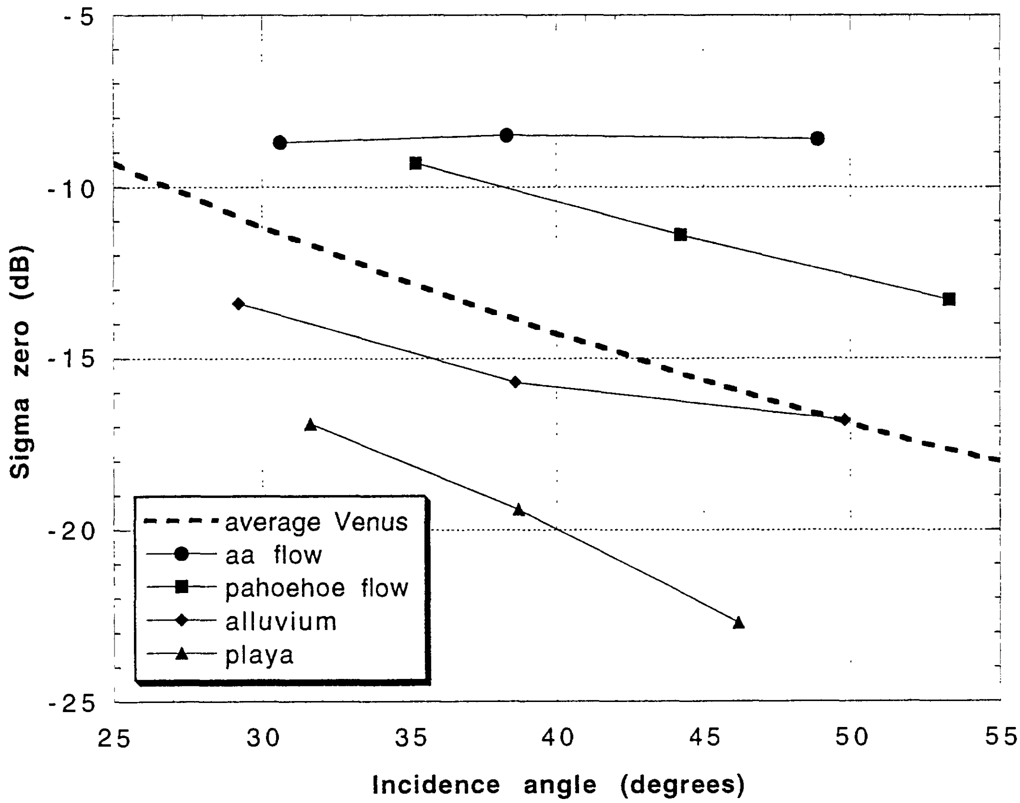

Figure 3. Normalized backscatter coefficient (also known as sigma-zero or σ_0) as a function of incidence angle for the average Venus surface and four terrestrial surfaces at 12.6-cm wavelength (after Plaut, 1991). Note that the aa flow, a strong diffuse scatterer, has large coefficients that are nearly independent of incidence angle, and the playa, a weak diffuse scatterer, has small coefficients that are a strong function of incidence angle.

The mapper's ability to identify linear features also depends on their orientations. Linear landforms that are transverse to the illumination or look direction are often prominent, but those that are parallel to the illumination or look direction may not be evident (see Wise, 1969; Yamaguchi, 1985). Other asymmetrical landforms, such as sand dunes, may be more evident in one look direction than they are in the opposite look direction because of their shapes. Similar phenomena may occur at scales that are finer than the resolution of the images (Plaut and others, 1992).

3. *Geometric distortion.* Geologic mappers should be aware that topography appears distorted in SAR images because of the translation of echo-time delay into horizontal distance. The effect is most noticeable for small features with large relief. Slopes that face the SAR antenna are foreshortened (or compressed), and those that face away are elongated (or expanded). Thus, peaks, hill tops, and crests of ridges are displaced toward the radar antenna in the look direction relative to their true positions. Distortion increases with decreasing incidence angle (see Ford and others, 1989, fig. 29). When the angles of radar-facing slopes exceed the incidence angle,

echoes from the tops of slopes are received before those from the base of the slopes; thus the relative positions of the tops and bases are transposed in the image (see Ford and Pettengill, 1992, figs. 4 and 5). The resulting transposition, called layover, is an extreme case of geometric distortion or relief displacement.

Although a minor nuisance to geologic mappers, geometric distortions in single images (monoscopic) can be used advantageously to estimate the relief and slopes of landforms that are symmetrical in the cross-track direction (Michaels, 1992, fig. 15). Foreshortening and elongation due to relief of landforms in different images of the same scene acquired with different incidence angles also provide a means of estimating with parallax measurements the relief of the landforms.

4. *Radar shadows.* Radar shadows are produced when no echoes are received because slopes are not illuminated by the SAR antenna. This effect is produced when slopes facing away from the antenna are greater than ninety degrees minus the incidence angle. Many slopes that face away from the radar have weak backscatter echoes and appear dark in the images, but true radar shadows are rare in Magellan images.

5. *Stereoscopy.* The principal value of stereoscopic viewing of image pairs of Venus is the enhanced ability to interpret landforms, structures, and geologic relations between rock units. Topographic relief can be perceived by simultaneous viewing of image pairs of the same scene acquired with different incidence angles because of the differences in geometric distortions or parallax. Such relief is best perceived when the image pairs have the same look direction but different incidence angles (see also Leberl and others, 1992). In some cases, relief can be perceived when the look directions are opposite.

Nearly all cycle 3 images are left-looking with smaller incidence angles than those of cycle 1 and can be paired with images of the same scenes for stereoscopic viewing. For most of these image pairs with north up, the image with the smaller incidence angle (cycle 3) should be viewed with the right eye and the image with the larger incidence angle (cycle 1) should be viewed with the left eye in order to attain the correct sense of relief. A reversed viewing arrangement is necessary for images of Maxwell Montes, where cycle 3 images have larger incidence angles than those of cycle 1. Mountains, hills, and domes appear to lean toward the antenna in the look direction. In attempts to view stereoscopically opposite-side images with north up, the left-looking image should be viewed with the right eye and the right-looking image with the left eye.

6. *Parallax relief.* Relief of landforms can be estimated because of the parallax engendered by different geometric distortions of landforms in image pairs of the same scene acquired with different incidence angles or look directions. Such estimates are particularly important for landforms and local relief at scale lengths that are too small for altimetry and for terrain that is complicated and difficult to decipher with altimetry.

Geometric relations and equations for making such estimates are illustrated for same-side or left-looking image pairs in figure 4 and opposite-side or right- and left-looking image pairs in figure 5. Of particular importance is the identification of "conjugate-image" points (the same points on the surface in each image of the pair). This identification is more readily achieved with same-side image pairs than with opposite-side image pairs. Measurements and calculations on digital displays in terms of pixels with subsequent translations to meters are recommended, but such measurements can be made with stereoscopes, parallax bars, and suitably oriented

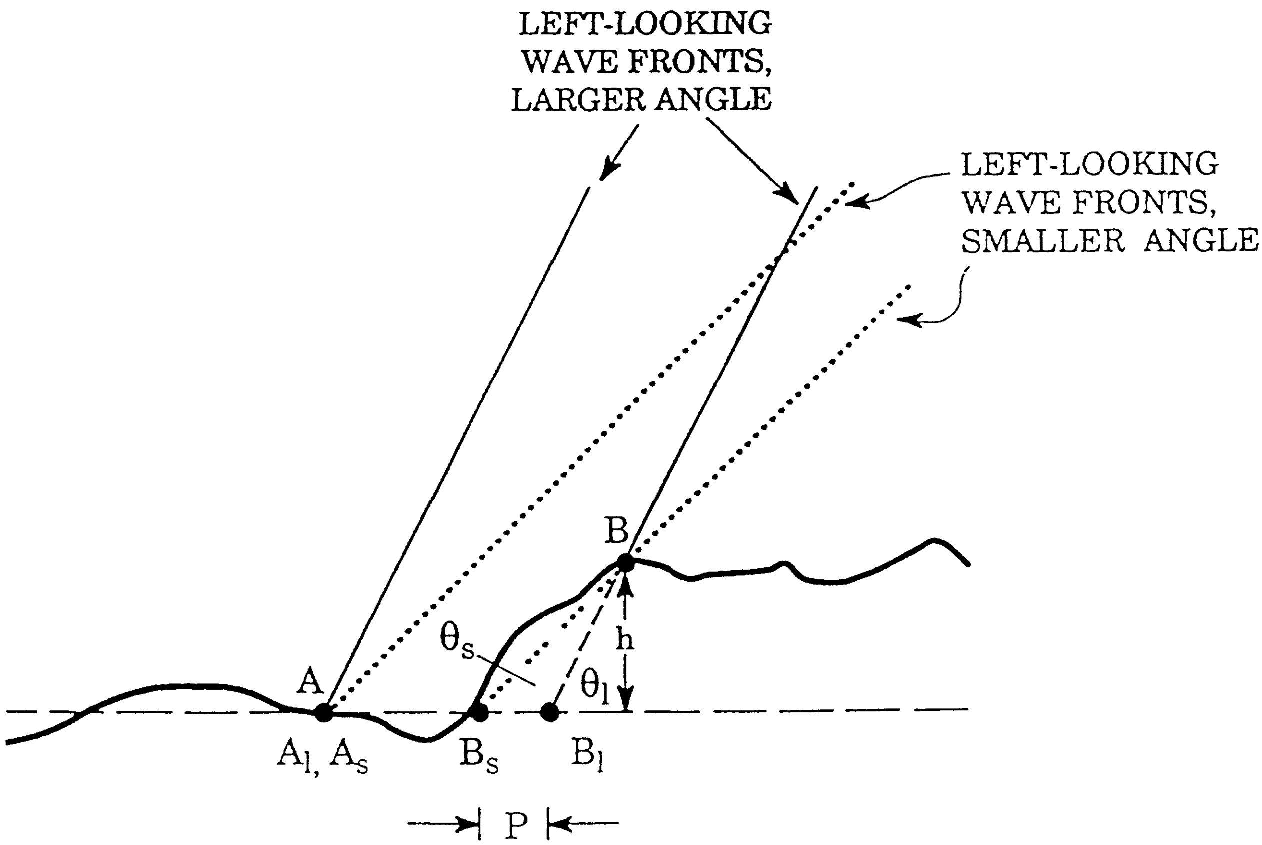

$$\text{PARALLAX (P)} = A_l B_l - A_s B_s$$

PARALLAX -HEIGHT RATIO (P/h)

$$\frac{P}{h} = \frac{1}{\tan\theta_s} - \frac{1}{\tan\theta_l}$$

Figure 4. Vertical profile of surface in the cross-track plane illustrating geometry of relief displacement and parallax for left-looking image pairs. A, a point on the surface at scale of image; A_s, point A in image with smaller incidence angle (usually cycle 3); A_l , point A in image with larger incidence angle (usually cycle 1); B, a second point on the surface at scale of the image; B_s, point B in image with smaller incidence angle (usually cycle 3); B_l, point B in image with larger incidence angle (usually cycle 1); Θ_s, smaller incidence angle; Θ_l, larger incidence angle; P, parallax; h, relief from A to B.

hardcopy images or their equivalents. It is also important to demonstrate that the look directions of the two images are roughly parallel, say within 10° of each other, because relief displacements are cross-track in the direction of the antenna.

Parallax measurements have been used to estimate the relief of lava flows (Moore and others, 1992), of crater rims above their floors (Schaber and others, 1992; Moore and others, 1993), and of volcanic edifices (Moore and others, 1993; Plaut, 1993). An excellent discussion of the method is given in Ford and others (1993).

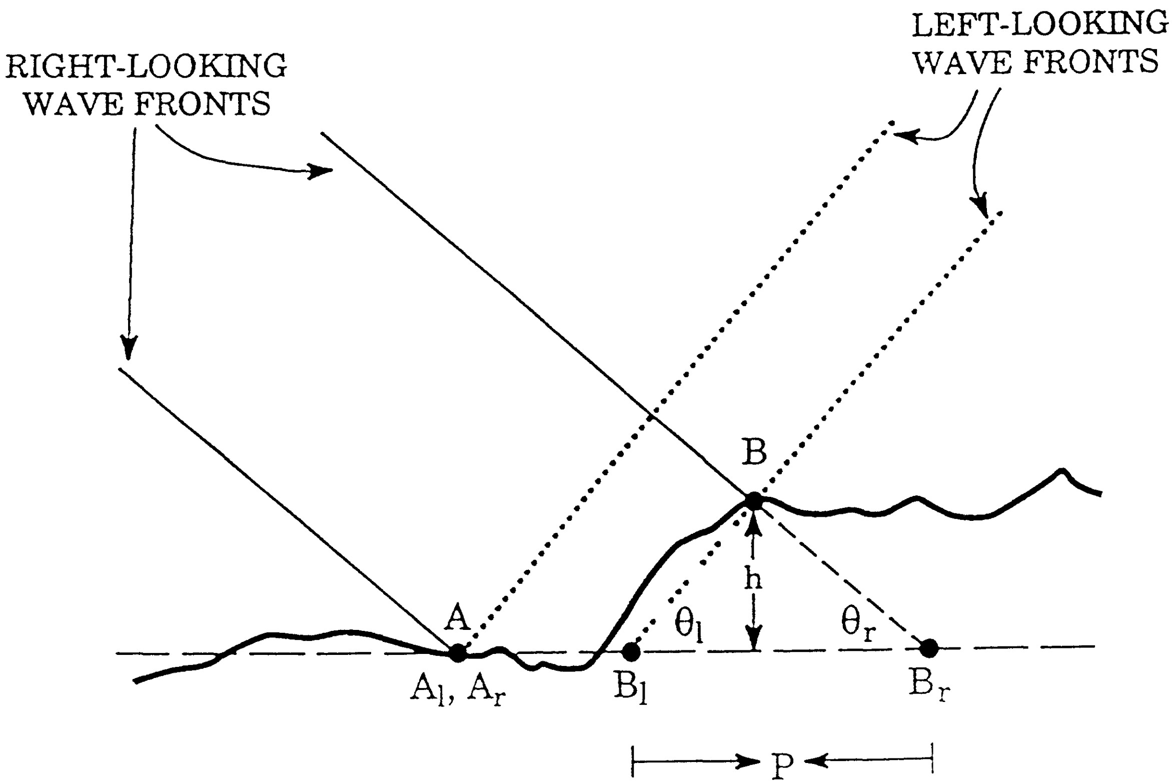

PARALLAX (P) = $A_r B_r$ - $A_l B_l$

PARALLAX -HEIGHT RATIO (P/h)

$$\frac{P}{h} = \frac{1}{\tan\theta_r} + \frac{1}{\tan\theta_l}$$

Figure 5. Vertical profile of surface in the cross-track plane illustrating geometry of relief displacement and parallax for left- and right-looking image pairs. A, a point on the surface; A_r, point A in image with right-looking incidence angle (cycle 2); A_l, point A in image with left-looking incidence angle (usually cycle 1 or 3); B, a second point on the surface; B_r, point B in right-looking image (cycle 2); B_l, point B in left-looking (usually cycle 1 or cycle 3); Θ_r, incidence angle of right-looking image; Θ_l, incidence angle of left-looking image; P, parallax; h, relief from A to B.

Some caution must be exercised in applying parallax measurements, because there may be significant image displacements related to navigational boundaries (differences in orbital parameters between uploads or each group of eight swaths). These displacements can be recognized by rotating the image pairs 90° and viewing them stereoscopically. Because of this problem, we recommend that parallax measurements be confined to small landforms or images that have been corrected for spurious image displacements. There are plans for correcting the Magellan images, but usable products may not be available in time for use in the Venus Geologic Mapping Program.

Altimetry. The nominal mission provided 3×10^6 altimetry measurements from between ±lat 85° with a vertical resolution of about 80 m. Cycle 2 measurements were halfway between those of cycle 1 so that more complete coverage could be attained. A global topographic dataset and a map with a 5-km pixel size have been produced from these measurements (Ford and Pettengill, 1992, plate 1). Overall, the Magellan altimetry data refined the general hypsometry of Venus (first determined by Pioneer Venus). Venus has a unimodal distribution of elevations; about 80% of the surface is within 1 km of the mean planetary radius (6051.84 km). Steep coarse-scale slopes (> 30°) are measured along the mountain fronts of Maxwell and Danu Montes and in Diana and Dali Chasmata in the equatorial highlands (Ford and Pettengill, 1992).

Altimetry data suitable for most geologic mapping are furnished to the mapper of each quadrangle in two forms: (1) in the same projection (Mercator, Lambert Conformal, or Polar Stereographic) as the mapper's quadrangle at 1:5,000,000 scale, and (2) a reduced color-transparency version of (1). A reduced-scale black and white transparency of the SAR image with the same scale and projection as the altimetry color transparency is also furnished to the mapper of each quadrangle to facilitate correlations and comparisons. The data are also available on CD-ROMs, which include global data sets in both sinusoidal and Mercator projections (GTDR.SINU and GTDR.MERC files) and ancillary data for those wishing more quantitative information; pixel size is about 4.6 km at the equator.

Reflectivity. Magellan coverage of Venus with reflectivity data closely matches that of the altimetry because both types of data are obtained from the same echoes. The Magellan data on reflectivity have systematic errors from an unknown source that cause the values to increase northward and southward from periapsis. Some data files have been empirically corrected for these systematic errors, but others have not (see below).

Normal reflectivity (for brevity, simply "reflectivity") is the ratio of quasi-specular echo power received from a surface at normal incidence and the power transmitted to the same surface. For Magellan, reflectivities are estimated by using the equation of Hagfors (1964; see for example, Tyler and others, 1992):

$$\sigma(\Theta) = (\rho\, C/2)\,(\cos^4 \Theta + C \sin^2 \Theta)^{-3/2}$$

where σ is the total cross section, ρ is the normal reflectivity, C is a surface-roughness parameter, and Θ is the incidence angle. $C^{-1/2}$ is interpreted as root-mean-square slope (see below). Diffuse scatterers on and at the surface effectively reduce the surface area available for quasi-specular echo scattering (Evans and Hagfors, 1964; Pettengill and others, 1988); some Magellan reflectivity data sets have been corrected for this effect by using SAR backscatter data (see below).

Of particular importance to geologic mappers are the relations between reflectivity and dielectric constant and model-dependent relations between relative dielectric constant and the physical-electrical properties of the reflecting materials. The relation between reflectivity (ρ) and relative dielectric constant (ε) is given by the Fresnel reflection coefficient:

$$\rho = [(\varepsilon^{1/2} - 1) / (\varepsilon^{1/2} + 1)]^2$$

Relative dielectric constant (also called dielectric permittivity) is the ratio of the dielectric constant of a material to that of free space or a vacuum.

There are a variety of model-dependent relations between the relative dielectric constant and physical-electrical properties of natural materials. Olhoeft and Strangway (1975) advocated the Lichtenecker mixing formula (see Saint-Amant and Strangway, 1970) and showed its applicability to lunar rocks and regoliths and their bulk densities; Garvin and others (1985) offered a modest modification to the equation of Olhoeft and Strangway. Campbell and Ulrichs (1969) applied the Rayleigh mixing formula to their data on dielectric constants and porosities of rocks, meteorites, and dry powders of these materials and cited references for other models. Selected relations are illustrated in figure 6 to give the mapper an appreciation for the significance of reflectivity.

Inclusions of electrical conductors, such as the mineral pyrite, in rocks and regoliths may have a profound effect on their dielectric constants (Pettengill and others, 1988). Rocks and regoliths containing such inclusions have been called "loaded dielectrics." This phenomenon may be an important factor contributing to the large radar reflectivities and low emissivities of Venusian surfaces at high elevations. The effects of conducting inclusions are presented by Pettengill and others (1988) and illustrated in figure 7.

Reflectivity data suitable for most geologic mapping purposes are furnished to the mapper of each quadrangle in a color-transparency with the same scale and projection as the SAR-image and altimetry transparencies mentioned above. The data are also available on CD-ROMs, which include global data sets in both sinusoidal and Mercator projections (GREDR.SINU and GREDR.MERC files) and ancillary data for those wishing more quantitative information; pixel size is about 4.6 km at the equator. It is important to realize that only the GREDR.MERC files have been corrected for both the systematic errors and diffuse scattering mentioned above (P.G. Ford, personal communication, 1992).

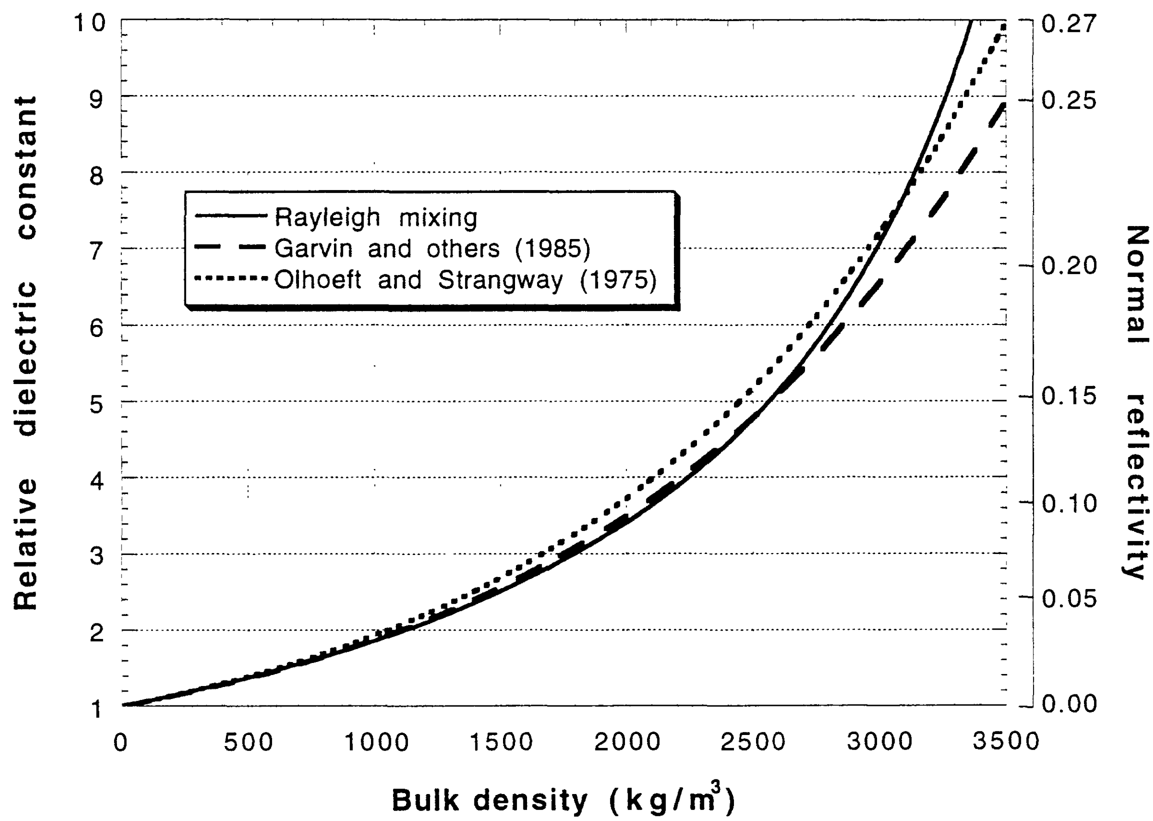

Figure 6. Relations between normal reflectivity and bulk density of rocks and dry rock powders or regoliths. Rayleigh mixing curve assumes a "parent rock" with a relative dielectric constant of 7.7 and a bulk density of 3,100 kg/m^3 (see Campbell and Ulrichs, 1969); curve extrapolated to a reflectivity of 0.25. Olhoeft and Strangway (1975) curve is based on experimental measurements of lunar rocks, aggregates, and regolith samples; light curves indicate one standard deviation. Relative dielectric constants (permittivities) calculated with the Fresnel reflection coefficient (see text). Conducting inclusions are not considered in these calculations.

Root-mean-square (RMS) slope. Quasi-specular echoes received by the altimetry antenna are spread or broadened in delay and Doppler frequency according to the probability distribution of tilted facets on the surface that are larger than the wavelength of the radar (about 10 to 250 wavelengths; see for example, Moore and others, 1980). Smooth, gently undulate level surfaces with small RMS slopes produce narrow echoes with sharp peaks. Rough, hummocky level surfaces with large RMS slopes produce broad echoes with broad peaks. To a crude approximation, RMS slope is analogous to the algebraic standard deviation of a slope-probability distribution. Regional surface tilts cause shifts in echo peaks from the delay and Doppler expected for level surfaces. Coverage of the Venusian surface is similar to that of the altimetry because both employ the same antenna. The mean RMS slope of Venus is 2.84°; values range from about 0.5° to 11° (Ford and Pettengill, 1992). A pair of slope-probability distributions of lunar maria samples derived from images and radar are illustrated in figure 8 to give the mapper an appreciation of the significance of RMS slope.

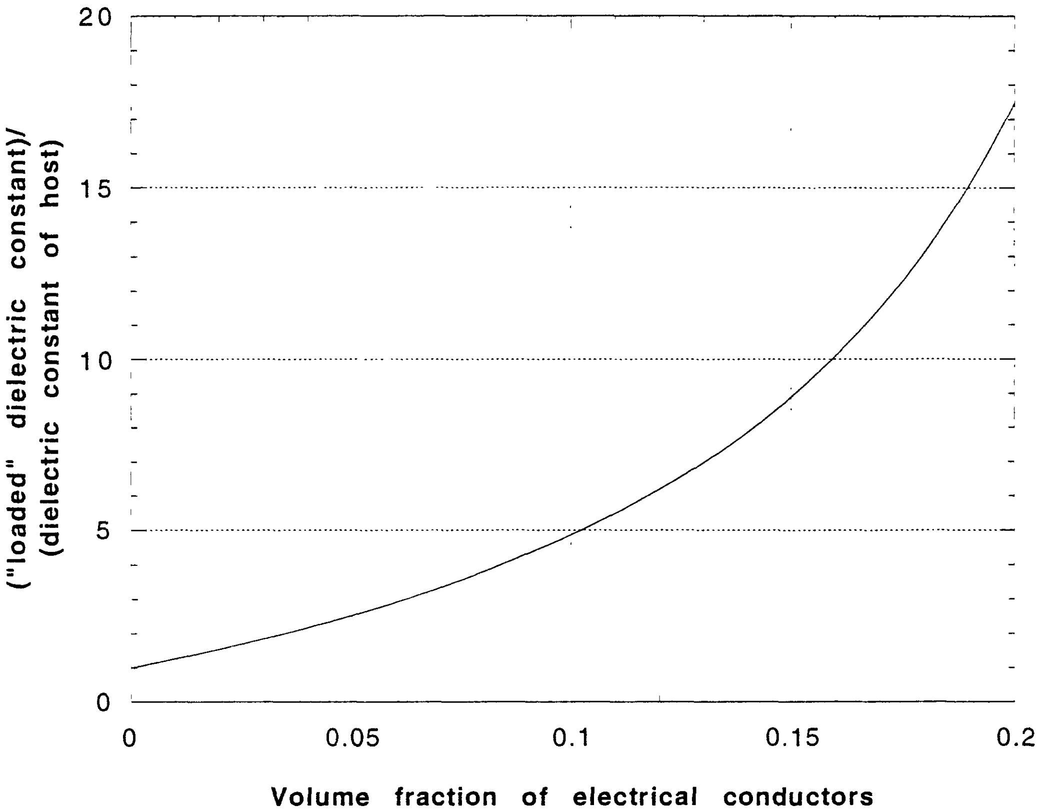

Figure 7. Relation between ratio of dielectric constants of a "loaded" dielectric and host material and the volume fraction of electrical conducting inclusions in the "loaded" dielectric (after Pettengill and others, 1988). For a volume fraction of conducting inclusions of 0.1, if the dielectric constant of the host is 5.0, the ratio is 4.87 and the dielectric constant of the "loaded" dielectric is 24.4.

Inversions of the delay and Doppler-frequency spectra show that the probability distributions of slopes of Venusian surfaces between 0° and 10° can be described with exponential, Hagfors, and Gaussian distribution functions (Tyler and others, 1992). In the analyses, contributions of diffuse echoes are justifiably assumed to be negligible. For nominal analyses (Ford and Pettengill, 1992), the echo spectra are fit with the Hagfors' scattering function noted above to obtain RMS slopes.

RMS-slope data from nominal analyses that are suitable for most geologic mapping purposes are furnished to the mapper of each quadrangle in a color transparency with the same scale and projection as the SAR-image, altimetry, and reflectivity transparencies mentioned above. The data are also available on CD-ROMs, which include global data sets in both sinusoidal and Mercator projections (GSDR.SINU and GSDR.MERC files) and ancillary data for those wishing more quantitative information; pixel size is about 4.6 km at the equator. The results of Tyler and others (1992) will be available on CD-ROMs in the future.

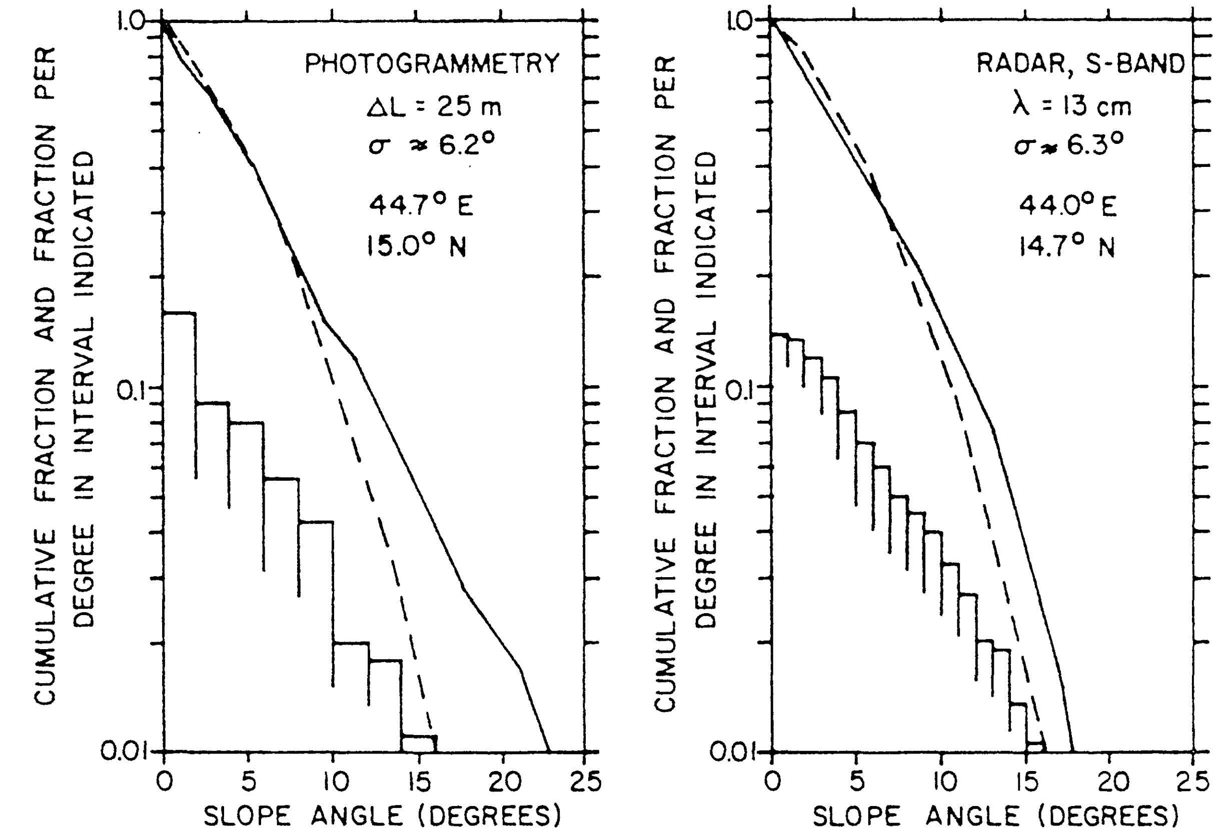

Figure 8. Slope-probability distributions of part of Mare Serenitatis obtained by using Apollo 15 panoramic camera photography and bistatic radar; (a) photogrammetry, 25-m slope length, and (b) bistatic radar, 13-cm wavelength. Incremental probability shown by bars, cumulative probability shown by solid line; hypothetical Gaussian cumulative probability for algebraic standard (σ) shown by dashed line. Note that actual cumulative curves are larger than Gaussian curves at large slope angles (reprinted from Moore and others, 1976, upper part of fig. 43).

Emissivity Emissivity (e) is the ratio of the radiance of a gray body and the radiance of a black body at the same temperature. For the hot Venusian surface and the frequency of the Magellan radar, the Rayleigh-Jeans approximation, or the ratio of the brightness temperature at 12.6-cm (T_b) and the physical temperature of the surface (T_p), is a close estimate of the emissivity (that is, $e = T_b/T_p$; see Schmugge, 1980; Pettengill and others, 1992, 1988). The mean emissivity of the Venusian surface at 12.6-cm wavelength is about 0.845 (Pettengill and others, 1992); the value is consistent with a dry, moderately dense, basaltic material. However, at elevations above about 6,054 km, most surfaces have very low emissivities (0.3-0.7) (Pettengill and others, 1992). Current explanations invoke elevation-dependent weathering processes that result in phase changes of inclusions of iron-bearing minerals to produce loaded dielectrics (Klose and others, 1992) or a material of average dielectric properties with many large voids that cause multiple scattering (Arvidson and others, 1992; Pettengill and others, 1992). The floors of some large impact craters also have low emissivities that result from compositional differences or other causes (Weitz and others, 1992). To an approximation, the Fresnel reflection coefficient (ρ) is the complement of the emissivity (e) (see Pettengill and others, 1988, 1991):

$$\rho = 1 - e.$$

This approximate relation between reflectivity and emissivity should be viewed with some caution, because the incidence angles for reflectivities (altimeter antenna) and emission angles for emissivities (SAR antenna) are not the same. Both reflectivity and emissivity are affected by surface roughness, and emissivity varies with incidence angle (Pettengill and others, 1992).

Emissivity data suitable for most geologic mapping purposes are furnished to the mapper of each quadrangle in a color transparency with the same scale and projection as the SAR-image, altimetry, reflectivity, and RMS-slope transparencies mentioned above. The data are also available on CD-ROMs, which include global data sets in both sinusoidal and Mercator projections (GEDR.SINU and GEDR.MERC files) and ancillary data for those wishing more quantitative information; pixel size is about 4.6 km at the equator.

Magellan Data Products

SAR image data records. Magellan radar data are processed and mosaicked into spatial image products to facilitate scientific analysis. The standard data products include image mosaics and ancillary data. Other special products include altimetric, rms slope, reflectivity, and radiometric datasets in image form for science analysis. A particularly useful portrayal is the superposition of color-coded datasets on the SAR backscatter data records (for example, Arvidson and others, 1991; Tyler and others, 1991; Kirk and others, 1992; Pettengill and others, 1992; Sandwell and Schubert, 1992). SAR mosaics are further processed to generate the scaled quadrangles that are used for map bases in the VMAP program. Both synthetic and real parallax stereopairs of Magellan image mosaics are being produced as well; the synthetic ones have parallax offsets generated by computer on the basis of Magellan altimetry data.

One Full-Resolution Basic Image Data Record (F–BIDR) was produced for each Magellan orbit; 1,790 orbits complete one mapping cycle (360° of longitude). (For the primary mission, solar conjunction prevented the return of SAR data for 110 orbits.) An additional 10 percent was lost during the nominal mission because of solar heating of electronic components (the spacecraft's solar reflectors had lost much of their efficiency), failure of one of the spacecraft's two tape recorders, and problems affecting spacecraft attitude. One F–BIDR contains nearly 60 Mbytes of 8–bit image data and less than 10 Mbytes of ancillary data. The F–BIDR format is 75 m/pixel resampled from the original ≥120-m cross–track and along–track resolutions and transformed into Sinusoidal Equal–Area projection; within 10° of the poles, the data are in oblique Sinusoidal projection (the F-PIDR format). Each F–BIDR forms a strip about 300 pixels wide by about 220,000 pixels long. In turn, about

30 F–BIDRs (or more at higher latitudes) are used to generate a mosaic, which has 7,168 lines by 8,192 samples. The mosaics are called Full–Resolution Mosaicked Image Data Records (F–MIDRs). Each F–MIDR is identified by center latitude and longitude and covers 5° of latitude and >5° of longitude (depending on latitude; see Michaels, 1992, figure 4). A "venetian blind" effect is commonly evident in mosaicked F–BIDRs because of border mismatches in backscatter intensity caused by minor errors in spacecraft pointing and navigation, in the topography model, and in processing.

To provide image-mosaic coverage for larger areas, the data are compressed in successive operations in which nine pixels are averaged and replaced by one pixel and then reprojected. The Once-Compressed Mosaicked Image Data Record (C1–MIDR) consequently has a resolution of 225 m/pixel and covers 15° of latitude and >15° of longitude (see Michaels, 1992, figure 5). In turn, successive compressions result in the 675 m/pixel C2–MIDRs (45° of latitude by >45° of longitude; Michaels, 1992, figure 6) and the 2,025 m/pixel C3–MIDRs (80° of latitude by >120° of longitude). Polar data records (F–PIDRs) and projections (P–MIDRs) portray areas at >80° latitude.

The various MIDR products are being distributed as photographic prints and digital files on CD–ROM disks. The CD–ROMs released by the Magellan Project are available to the planetary geoscience community through the National Space Science Data Center in Greenbelt, Maryland.

Synthetic stereopairs and merged databases. Synthetic parallax stereoimages of most of Venus based on C1–MIDR image mosaics have been produced by the U.S. Geological Survey for the Magellan Project as preliminary tools in assessing the global geology of Venus. These synthetic stereoimages are produced by (1) geometrically registering to a single Magellan image mosaic the best available altimetry dataset (8 x 11 km to 20 x 29 km resolution, depending on spacecraft altitude), and (2) introducing parallax into the MIDR, as controlled by the registered geometry (that is, shifting pixels left or right by a distance proportional to the altitude relative to the average altitude in the MIDR, so that the overall average shift is zero pixels). Vertical exaggerations have been produced at 10X and 50X. These stereoimages will be important for interpretations of the broad topography, which will be valuable in analyzing the larger landforms associated with volcanism and tectonism.

In addition, perspective views can be generated from the merged topography and SAR image mosaics. Other radar databases (emissivity, reflectivity, rms slope, etc.) can be colorscaled and combined with black-and-white SAR mosaics for normal or perspective views or for synthetic stereo analysis.

Map projections. To assist in various cartographic endeavors, formal map series are being produced at various standard scales and projections. Such maps will be used as base materials for geologic mapping. The VMAP program is sponsoring geologic mapping of the 1:5,000,000–scale series that consists of 62 quadrangles (fig. 1). The series includes Mercator (<25° latitude), Lambert Conformal Conic (25° to 75°), and Polar Stereographic (>75°) projections. All are conformal projections, which retain the approximate shape of small landforms. However, all are distorted across larger regions. The Mercator base, visualized by a cylinder perpendicular to the equator, is conveniently rectangular, but scale changes rapidly with latitude (Batson, 1990, fig. 3.1). For Venus, the cylinder intersects at ±15.9° latitude, where the true 1:5,000,000 scale occurs. The Lambert Conformal Conic projection is represented by a cone tangential to the globe whose apex intersects the spin axis of the planet (Batson, 1990, fig. 3.3). The latitudes of cone–globe intersection are called standard parallels. Scale changes with latitude. For Venus, two rows of these projections occur in each hemisphere with standard parallels at 34° and 73°, where true 1:5,000,000 scale occurs. Polar Stereographic projections represent planes tangent to the axial pole (where true scale occurs). The scales of the projections are the same where they join (at lats ±25° and ±75°).

Other map series that are being produced for Venus contain 340 sheets (Sinusoidal) at 1:1,500,000 scale, 8 sheets (6 Mercator and 2 Polar) at 1:10,000,000 scale, 3 sheets (2 Mercator and 1 Polar) at 1:25,000,000 scale, and 1 sheet at 1:50,000,000 scale. For more information, refer to Batson (1990).

Non-Magellan Radar and Other Data

Since the early 1960s, Venus has become one of the planets most visited by spacecraft. Fifteen Soviet and six U.S. missions have probed its sulfurous clouds to measure atmospheric structure and composition. Other investigations disclosed a lack of water vapor and the absence of a magnetic field. Seven of the Soviet craft were landers that conducted chemical analyses of rocks, which indicated that some have compositions similar to basalt and thus may be of volcanic origin. One of the landers, Venera 9, gave us our first glimpse of the surface when, in 1975, it relayed a panoramic view. These early explorations were enhanced by observations in the field of radio astronomy that indicated that Venus is a perpetual furnace; surface temperatures reach 482 °C (~900 °F), and the atmospheric pressure is 90 times that of Earth's (Young, 1990).

The 1978 U.S. Pioneer Venus Orbiter (PVO) was the first spacecraft to carry a radar (SAR-type) sensor to Venus, and the altimetry of 92 percent of the surface was mapped at a resolution of 50 to 140 km. For the first time, planetary scientists had a global map of Venus. Continent-size highlands, hilly plains, large mountains looking like volcanoes, and flat lowlands were revealed (Masursky and others, 1980). Much of the initial scientific results from the Pioneer Venus mission were published in a special issue of the Journal of Geophysical Research dedicated to that mission (December 1980, v. 85, no. A13, p. 7575-8337).

Five years after Pioneer Venus went into orbit, the Soviet Venera 15 and 16 spacecraft used radar to map about 25 percent of Venus (lat 25-90° N.) at a resolution of 1.2 to 2.4 km. These images revealed evidence of abundant volcanism, impact craters, and complex tectonic deformation, including coronae—large, oval features of apparent volcanotectonic origin previously unrecognized on other bodies in the Solar System (Kotelnikov, 1989). The geoscience investigations of Venera 15 and 16 are described in many publications (see Recommended Reading).

Earth-based radar observations of some regions of Venus have been made primarily from the Arecibo Radio Observatory and the Goldstone receiving station since the mid-1960s (see, for example, Jurgens and others, 1980, 1988a, b; Burns and Campbell, 1985; Campbell and others, 1989, 1990; Campbell and Campbell, 1992; Plaut and Arvidson, 1992). The Goldstone radar coverage is restricted to lat 23° S. to 23° N. and long 260° to 32° E. (Plaut and Arvidson, 1992), while that from the Arecibo Observatory is limited to most of the area between lat ±67° and long 265° to 35° E., about 23 percent of the surface (Campbell and others, 1990). In all, about 40 percent of Venus has been mapped from these radar stations (Campbell and others, 1990).

GEOLOGIC MAPPING OF VENUS

The basic objective of the coordination efforts of the Venus Geologic Mapping Program is to ensure that the geologic maps have reasonable consistency (such as in usage of map–unit names and map symbols) and agreement, which will provide a useful basis for geologic interpretation. Mappers should be guided not only by fundamental geologic principles, but also by many precedents and approaches (some more applicable to Venus than others) that have been established through previous planetary mapping programs and various early mapping studies of Venus. (See Recommended Reading; in particular, the book chapter by Wilhelms (1990) should be regarded as *essential* reading.) In addition, mappers will face the new challenges of the distinct geologic character of Venus, broadly and in detail, and of the nature of the radar datasets. Mappers should follow guidelines of the USGS; even though adherence to basic mapping principles is a must, mappers have considerable latitude in their application and are encouraged to investigate new approaches that may result in a more instructive and useful geologic map. For example, structurally complex terrains generally cannot be mapped as conventional rock (material) units; inclusion of terrain units may necessitate altering their depiction on correlation charts and cross sections. Also, additional small-scale maps depicting major tectonic structures or surficial features may be necessary to depict the geology of complex regions clearly and comprehensively.

Rationale and Methods

Defining map units. Map units will be defined on the basis of various morphologic, textural, and structural characteristics observable in Magellan images. *Geologic (or rock or stratigraphic) units* are made up of bodies of rock that are thought to have formed by a particular process or set of related processes over a discrete time span. Even though the interpretation of a map unit or its relative age may not be clear, the unit must have distinctive characteristics. Some surface rocks, however, are so modified by processes postdating their emplacement that their original key characteristics no longer are decipherable. In many of these situations, it is impossible to define geologic units with confidence. Rather than leaving the map blank, it is appropriate to map *geomorphologic units* that are based on the same types of characteristics, even though the characteristics developed much later than the emplacement of the modified rocks (see Milton, 1975). Where particular morphologic structures or other associated features are rare, the mapper should choose simply to discuss them in the unit description and perhaps map them as symbols rather than delineate a new unit based on them.

Some mappers may find that a different approach to defining map units is more suitable for their Venusian quadrangle. In particular, *tectonic units* should be considered. Until now, planetary maps have generally excluded tectonic mapping as has been practiced for the Earth. Tectonic mapping has been varied and highly subjective because of changes in paradigms used to interpret and understand terrestrial tectonics. Actually, mapping styles once used for the terrestrial continents—styles that predated our understanding of plate tectonics—appear most applicable to Venus, because they distinguished rocks and terrains associated with foldbelts and cratons (see King, 1969a, b; King and Edmonston, 1972). King promoted a relatively conservative style (although much of the terminology of his day is losing favor among geologists). He stated (1969b, p. 87) that a tectonic map "portrays the architecture of the upper part of the earth's crust, or the features produced by deformation and other earth forces, and represents them by means of symbols, patterns, and colors." Recently, because plate tectonics has gained wide acceptance because it explains much of terrestrial tectonics, the mapping of *tectonostratigraphic terranes or elements* has become popular (for example, see volume edited by Howell, 1985). Such units are understood to be fault bounded and defined according to stratigraphy, tectonic disruption, or metamorphic overprint. Small-scale mapping of these units caters to accretionary plate tectonics (see Howell, 1985, map insert; Dickinson and others, 1986).

Units should be mappable on Magellan SAR backscatter image mosaics, which form the primary dataset that permits identification of morphology and structure. Unit descriptions should be augmented by radar characteristics such as radar "brightness," backscatter coefficients, emissivities, reflectivities, rms slopes, and topography from altimetry (for example, see Arvidson and others, 1992, fig. 7 and table 1; Moore and others, 1992, table 3). However, mappers should avoid defining units solely by such characteristics, which may be related to weathering or deposition of thin eolian or impact material and have little or nothing to do with the emplacement or structural modification of the affected map unit (Arvidson and others, 1992; Greeley and others, 1992). Also, the nonbackscatter radar data seldom clearly define mappable areas because of their common variation with respect to surficial rock properties and relatively low resolution. Where stereopairs are available, stereoscopy adds the important dimension of local relief for characterization of geologic units at a scale that is not possible with Magellan altimetry or synthetic stereopairs; stereoscopy enhances geologic mapping and interpretation to a degree that cannot be overestimated.

Units may have distinct contacts, perhaps expressed topographically or by cross–cutting and overlap relations. Where contacts are indistinct, mappers may make them long-dashed or queried (which signifies, respectively, gradation or uncertainty). Alternatively, mappers may redefine the observational basis that distinguishes the units. As a last resort, units can be lumped.

Correlating map units. Contacts between map units are critical in defining emplacement relations and relative ages and should be clearly presented on the map. Contact geometry may suggest overlap, embayment, crosscutting, or abutment relations that may be used to infer relative age. Structural relations may also be useful in determining relative age.

On Venus, relatively late resurfacing and a thick atmosphere have resulted in crater densities that are too low for detailed stratigraphic work; thus far, only 921 impact craters have been identified on about 98 percent of the surface. Over broad areas of Venus, crater densities are spatially random (Schaber and others, 1992), although lower than average densities of some areas are interpreted to be related to extensive volcanic resurfacing and tectonism (Phillips and others, 1992).

The global chronology of Venus will be determined through the collective efforts of the geologic mappers, who will establish the local geologic history within their individual map areas. Time markers may include widespread geologic and geomorphologic units, structures, and surficial signatures related to impact events or weathering (Izenberg, 1992; Tanaka and Schaber, 1992).

Mapping approach. (This section is largely distilled from Wilhelms, 1990, section 7.4.) Initial familiarity with the map area is achieved by reconnaissance mapping. This first step reveals the overall geology and identifies major map units, their stratigraphy, and structures. To explain the geologic evolution of the area, working hypotheses are formulated that can be tested and revised as more detailed mapping proceeds. The reconnaissance also assists in identifying the most significant and challenging problems in the area, whose resolution will be the major objective of the mapping.

Detailed mapping is best started where units and contacts are most clearly mappable. Commonly the location is determined by the availability of the highest resolution data. Thus, where FMIDRs are available, they can be individually used for mapping in greater detail than can be shown on the quadrangle, which will provide the mapper with a more complete understanding of the local geology. Another approach is to map younger units first—these units are generally better exposed, and their relative age relations are easily portrayed. A working set of map units and symbols is generated and then modified as mapping progresses. Where key features (such as small volcanoes) are too small to map as units, they may be portrayed as map symbols. Ultimately, the level of detail shown on the maps will be dictated by scale and perhaps ancillary data such as stereopairs and FMIDRs.

Other datasets can be incorporated in the mapping as appropriate, including SAR backscatter cross section, topography, emissivity, reflectivity, and rms slope. However, radar characteristics in most cases constitute a poor basis for unit definition because of their dependence on surficial properties. Some units may even be difficult to map consistently on the basis of SAR backscatter, because backscatter intensity varies according to incidence angle and, in some cases, look direction. If mapping of surficial characteristics is desired, it should be regarded as secondary in importance to mapping of geologic materials and structure and shown in a separate map figure.

As in traditional field mapping, note-taking is vital in documenting the mapping procedures and approach used and in highlighting key geologic observations and relations. Such observations include morphologic characteristics, overlap and cross-cutting relations, and evidence for style and sense of structural deformations. A notebook dedicated solely to the map is very valuable; in it, extended notes can be located by annotations, perhaps on a map overlay. Such documentation contributes to the production of a thorough, well-balanced, consistent, and insightful interpretation of the geology of the map area.

After an initial set of associations and age relations among map units has been derived, a correlation chart consisting of boxes for each map unit can be developed. Map units generally lend themselves to grouping according to terrain type or geologic or geographic associations. Hierarchic names include many possibilities that reflect what the units have in common, such as terrain type (for example, plains, plateaus, mountain belts, shields, and canyons), perhaps subdivided according to local individual geographic features. When the association is based on a geographic feature, the name of the feature coupled with descriptive terms such as "assemblage" or "sequence" will form the hierarchic name. Relative ages of the map units are represented on the correlation chart by vertical position. Thus units that are clearly younger should be shown above older units; those that overlap in age will have boxes that overlap vertically. Because some units developed over a considerable timespan, their boxes may be much longer than those of other units. For a poorly defined age limit, a sawtooth box edge should be used. Boxes for closely related units share a box edge that is horizontal or vertical as appropriate; where their ages overlap, they may share a diagonal box edge. (See examples of planetary geologic maps cited below.) Where geologic and structural relations are complex, informal cross sections can be attempted as tests of possible scenarios of development. Preliminary correlation charts and cross sections are excellent tools to identify areas and relations that require more careful examination.

Coloring the preliminary map as parts are completed is the best way to identify incomplete contacts, incorrect symbols, and inconsistencies in mapping style. Other special maps, perhaps of selected areas at larger or smaller scales, may be used to show tectonic structures or surficial materials and features. Such maps not only highlight specific aspects of the geology, but they also may reduce the clutter on the primary geologic map. In a few instances, particularly in areas of high relief, a schematic cross section can be added to interpret structure; these sections generally have a vertical exaggeration, which is stated.

When the mapping is complete, the description of map units (DOMU) and text can be written. The DOMU describes the map units shown on the correlation chart according to groupings in the hierarchy, from youngest to oldest (in reverse chronologic order—opposite the oldest-to-youngest order used in the text's discussion of stratigraphy). Descriptions and interpretations of units are always clearly separated. The description should include the unit's physical characteristics, occurrence, and relations with other units. The interpretation may include the inferred rock type and mode of origin of the unit; multiple interpretations may be included. Map symbols are explained after the DOMU. The map text should include an introduction that describes the basic geologic setting and physiography of the map area, relevant previous work, objectives of the mapping, and constraints of image resolution that may have affected it. The body of the text should reconstruct in detail the geologic history (from oldest unit to youngest) on the basis of map relations and interpretations. However, the discussion should not include directed, refined geologic analyses typical of those found in research articles.

Types of Mapped Units and Features

Prior to Magellan, small-scale (1:15,000,000) geomorphologic mapping of the northern quarter of Venus was based on kilometer-resolution radar mosaics imaged by the Venera 15 and 16 SARs (Sukhanov and others, 1989; Schaber, 1990; Schaber and Kozak, 1990). At that resolution, many important geologic (especially stratigraphic) relations were not discernible. However, the higher resolution Magellan data permit more detailed and "classic" stratigraphic and structural mapping and interpretation, as can be seen from examples in recent journal articles. These various examples are useful in visualizing how map units can be defined and how contacts and various structures can be mapped. (Keep in mind that the published examples use various names and conventions that may or may not be appropriate for VMAP). This section is divided into discussions of the major types of terrains and structures to be mapped on Venus.

Plains materials. Plains units generally are characterized by relatively smooth-appearing (at image resolution) surfaces at low to intermediate elevations. Relative ages are determined by embayment and cross-cutting relations. Units can be subdivided according to morphology (for example, smooth (at pixel scale), ridged, hummocky, fractured, complex); geographic and terrain associations; relative stratigraphic position (such as lower, middle, and upper); and, *locally*, radar brightness (for example, bright, dark, mottled; see Solomon and others, 1992, fig. 32);

Lava flows and volcanoes. In some areas, individual or multiple lava flows can be subdivided according to radar brightness, superposition, morphology, and surface texture (for example, Arvidson and others, 1992, fig. 6; Head and others, 1992, fig. 9a, d; Moore and others, 1992, fig. 4; Senske and others, 1992, plate 1). Large volcanoes may have distinctive and mappable summit or central caldera areas and associated structures (Head and others, 1992, figs. 3a, b, 4a–c, 5b; Senske and others, 1992, fig. 6). Small volcanic shields or domes may be outlined individually (Head and others, 1992, figs. 2b–d) or shown by point symbols. In some areas, flow directions can be indicated.

Structural terrains and features. The greatest challenge faced for many of the VMAP quadrangles is the mapping of structural terrains and features. A common mistake is to draw in as many structures as possible; this approach results in clutter and is not helpful to the reader. (Remember that the quadrangle base will portray much of the character of highly deformed map units.) Instead, map highly deformed terrains as units and trace only particularly significant or representative structures on the geologic map (compare King and Edmonston, 1972; King, 1990a). Structural terrains include ridge and fracture belts, tesserae (or complex ridged terrains), and other highly deformed areas. These terrains may be delineated on the basis of elevation, relief, dominant structural type(s), structural patterns, size of individual structures, and structure density (Solomon and others, 1991, figs. 7D and 8B; Bindschadler and others, 1992a, figs. 3–7; Fienen and others, 1992). Care will be needed in areas where structural characteristics change gradually; if units are not sufficiently distinct to map separately, it may be better to lump units and show gradational trends through the mapping of representative individual features.

Significant individual features can be mapped by symbols (see Appendix B). Many mappable Venusian features are tectonic structures; however, topographic features (ridges, troughs, depressions, and scarps) and erosional features (channels) also are common. Mapping of faults or folds requires some supporting evidence for the deformation (such as offset surfaces). If such evidence is absent, a dashed or queried symbol, a less interpretative structural feature (for example, fracture instead of fault or graben), or a topographic feature (ridge instead of fold) can be mapped instead. Regional structures may be distinguished from local structures on the map by a heavier line weight.

Many geologic mappers will find it advantageous to represent both detailed structure and large tectonic features on a separate base at a similar or smaller scale. For example, coronae and coronalike features differ greatly in structural detail (Stofan and others, 1992, figs. 2–5, 13). Even so, detailed structural mapping may be tedious (Head and others, 1991, fig. 7D; Squyres and others, 1992a, fig. 4c). Instead, representative features may be mapped and perhaps summarized by rose diagrams where appropriate (Head and others, 1992, figs. 5–8; Senske and others, 1992, figs. 9–12, 16, 17, 20; Squyres and others, 1992a, fig. 8d; 1992b, figs. 5 and 7). Simplified, smaller scale tectonic maps may also be drawn (see Senske and others, 1992, figs. 4, 19, 21). (All graphs and line work will be redrawn by the USGS Office of Scientific Publications, but mappers should follow guidelines in Hansen, 1991.)

Impact craters. A special type of structure shown on most planetary maps is the impact crater. On other bodies, generally only larger craters are mapped, consistent with map scale. But, because only about 900 craters are recognized on Venus, they are all significant and should all be mapped. However, craters smaller than about 20 km in diameter may have to be indicated by a map symbol. In addition to the crater rim crest, the outer boundary and facies of impact ejecta, floor material, secondary craters, ring structures, central peaks, and outflows can be mapped in many cases (Schaber and others, 1992, figs. 23, 25–27). Also, mappers may choose to subdivide craters into various morphologic classes (for example, Schaber and others, 1992, fig. 4). Extensive surficial features associated with craters (such as dark splotches) should not be mapped as geologic units, but they may be shown by stipple patterns or in a separate, reduced-scale figure.

Mapping Conventions

Unit names, letter symbols, and colors. (See also Wilhelms, 1990; Hansen, 1991, p. 43–52; Reynolds and others, in press.) The general practice in planetary mapping is to use descriptive informal names (such as crater material, ridged plains material, or fractured highlands material). Informal names should include a term that shows that the unit is either a material (geologic) or surface (geomorphologic) unit. Formal names are occasionally applied to stratigraphically distinctive or complex rock units in planetary geology (for example, "Medusae Fossae Formation" on Mars); a formal name requires a formal definition following as closely as possible the established guidelines of The North American Commission on Stratigraphic Nomenclature (1983) (see Hansen, 1991, p. 44–49). We discourage the use of formal names in early stages of mapping a planet, however, because experience shows that many unit definitions and portrayals change substantially through the course of several years of research. We also discourage use of jargon (for example, "tick"), because of the resulting confusion to general readers.

As in terrestrial mapping, the unit-letter symbol is an abbreviation of the unit name. Because a formal stratigraphic system has not yet been established for Venus, no capital letter representing a time–stratigraphic system will be included. The symbol should have as few characters as possible. Avoid ambiguous usage (for example, use *p* for plains and *pl* for plateau). The letters should be arranged such that the basic formational name is followed by modifiers for members and submembers (for example, "lower ridged plains material of the Artemis assemblage" would be "unit aprl"). Some mappers identify a sequence of unit members by subscripts, the stratigraphically lowest unit being designated 1. (Thus member 1 of the example given above would be "unit $aprl_1$.") In the map text, a unit's name is always used, with or without its letter symbol; the symbol never stands alone. A symbol may be queried on the map (for example, "aprl?") if the unit assignment is in doubt; the reason for the doubt should be given in the DOMU.

The Venus Geologic Map Series will follow a consistent color scheme to the extent possible. Colors on the published maps are limited by the USGS color palette and will be selected by the map coordinator. However, authors should adopt the following general guidelines on their author–colored ("mill") copies—*browns* for older or heavily deformed terrains and units, *purples* for less heavily deformed terrains, *greens and blues* for plains units, *reds and oranges* for volcanic materials, *yellows* for craters, and *grays* for other materials. In addition, stippled overlays can show surficial units, broad tectonic zones, etc., that are superposed on the other map units. Some variation from this scheme is occasionally warranted where many subdivisions of units are made and a wide selection of color shades is not available. In general, maps are more visually pleasing and easier to read if the areally large map units are represented by light shades (pastels) and the small, patchy units are darker or more intense. Also, the colors of adjacent units should display sufficient visual contrast so that they do not become confused. Areas of missing data will be left uncolored.

Line and point symbols. A host of line and point symbols is available to the mapper; where possible, symbols should be those standardized by the USGS for terrestrial maps (Reynolds and others, in press) or those used on published USGS planetary maps (such as those used for crater rims). Many of the symbols used on planetary geologic maps are shown in Appendix B. (If a new symbol is needed, the VMAP Coordinator should be consulted.) Symbols need to be used judiciously to reduce map clutter. Thus, mapping of most secondary morphologic features such as fractures, wind streaks, yardangs, or channels should be avoided or done sparingly; for example, one large arrow (rather than several small ones) can often be used to show flow direction. In many places topography will be visible on the SAR backscatter base of the published geologic map. If the mapper wants to highlight specific features, they may be shown on a supplementary map at reduced scale.

Although structural symbols are desirable and informative, their application in some cases may be highly conjectural and uncertain. Thus fault symbols should be avoided except where offset is evident or probable. Normal faults, grabens, and some strike–slip faults may be acceptable. However, suspected thrust–fault scarps and folds should generally be mapped as queried, dashed, or as topographic symbols (scarps and ridges); their structural interpretation can be discussed in the text or shown in cross sections.

Geographic names. The mapper will be provided with an index map showing all named features in the map area. Only geographic names officially approved or provisionally accepted by the International Astronomical Union (IAU) can be shown on the map or mentioned in the text; a name's provisional status must be indicated, usually by an asterisk after the name on the map. Reference to unnamed features should be made by latitude and longitude (all features mentioned in text or DOMU, if not shown on map or in figures, must be located by map coordinates). Note that many craters, coronae, and other geographic features do not have names (see Schaber and others, 1992, table A1; Stofan and others, 1992, table 1). If you feel that a feature needs a name, please consult with the USGS representative to the IAU; guidelines for naming features are given in Appendix C.

MAP COMPILATION, REVIEW, AND PUBLICATION

Careful, thorough map-compilation procedures help avoid inaccuracies; inconsistencies between the map, text, and DOMU; and an unbalanced portrayal of the geology. The use of general procedures and style guidelines established by the USGS for the submission, review, and editing of planetary maps will materially expedite review and publication of maps. In addition, discussions with and informal reviews by authors of adjacent maps permit amicable and informal resolution of differences *before* a map is submitted. A USGS convention requires that map borders match those of neighboring maps submitted earlier, and texts should agree with neighboring texts, *unless* the author of the later submittal explicitly justifies the differences.

Compilation

VMAP mappers will compile their work on a mylar (stable-scale) base registered to a quadrangle base at 1:5,000,000 scale; corner points will be marked or holes registration punched. A subdued half–tone version (or "brownline") of the map base on mylar will be supplied for drafting map contacts and symbols. Other available image databases, including left- and right-look SAR mosaics, altimetry (including synthetic stereopairs), and emissivity data, will be supplied to the mapper. Geologic mappers must prepare not only the geologic map but also supplementary charts, figures, and text that include (1) a correlation chart, (2) a discussion of the geologic history of the map area, including specific results and interpretations of stratigraphy, structure, and other geologic features and relations (with a reference list and optional acknowledgments, figures, and tables), and (3) a description of map units and symbols. Cross sections and supplemental, special–purpose maps (generally at reduced scale) are optional. Supplemental information about the map base (including an index map, scale, and cartographic notes on base) are not the author's responsibility; they are added by USGS cartographers and drafters.

Mapping is compiled on the half-tone cronaflex quadrangle base. The emulsion is on the back side of the cronflex, so that erasures of drafted work on the front side do not affect the mosaic. Preliminary reconnaissance mapping on a paper print or mylar overlay prior to final compilation on the brownline base can be very helpful. The submittal copy on the cronaflex base should be drafted in ink. The line weight for major structures should be clearly heavier than that used for contacts, but minor structures can be shown in a light line weight. Prior to submittal, the *mapper* should color a paper ozalid or photocopy of the brownline to ensure proper and complete labeling of units. At the same time, all intersections of three map units should be checked; contacts should be drawn to reflect correct relative age (younger rock units should embay older ones; erosional geomorphologic units should crosscut the eroded units). Coloring the younger units first will readily expose any mistakes in the portrayal of overlap relations. *Every outcrop* is given a letter symbol; not only are these labels helpful to reviewers, but they prevent drafting errors. (Later on, the colorproof and published map will not bear so many labels because "color carries," but at compilation stage the extra precautions are necessary.) Also, the positions of all line and point symbols have to correspond precisely with the location of the feature on the base (the drafters will attempt to follow precisely the *author's* linework). Other illustrations involving map units (correlation chart, special maps, figures, and cross sections) should also be colored and checked for similar errors and inaccuracies; for example, cross sections have to match the map at the surface and mapped stratigraphic relations must agree with those shown in the correlation chart.

The author should also carefully check for consistency among the map, illustrations, and explanation and text. Many times unit occurrences are discovered to be incompletely described or unit names and symbols inconsistently rendered. Another common inconsistency is to make lengthy one-sided arguments regarding the interpretation of a few units or structures. A more complete listing of common problems in geologic maps is given by Wilhelms (1990, section 7.4.9).

USGS manuscript-preparation guidelines should be followed. Extensive changing of the format of your manuscript to adhere to guidelines after preparing it can be a frustrating experience. Instructions for the format of map texts and DOMUs are provided in Appendix D.

Pay particular attention to following telegraphic style for the explanation, in which both definite and indefinite articles and forms of the verb "to be" are omitted and the map unit is understood as the primary subject. The unit's characteristics should be described first, from primary to secondary ones, followed by geographic occurrence (if not obvious on the map) and relations and associations with other units. Finally, the interpretation is set off at the end. For example:

> Ridged plains material—Forms smooth plains marked by northeast–trending wrinkle ridges; fractures and flow lobes rare; generally radar dark. Overlaps highly fractured unit of Artemis Chasma; buried along south edge by lobate plains material. *Interpretation:* Low–viscosity lava flows erupted from local fissures; deformed by compressional stresses related to development of Artemis Chasma

Mappers will also benefit from familiarizing themselves with relevant guidelines in Hansen (1991): "Preparing Maps and Other Illustrations" (p. 184–211) and "Formatting Survey Manuscripts for Review and Editing" (p. 250–264). The first of these sections provides guidelines primarily for terrestrial maps, thus it is advisable to examine recent planetary maps for format and style unique to them. Some informative examples are the geologic maps of (1) the western equatorial region of Mars (Scott and Tanaka, 1986), which has an extensive and complex correlation chart; (2) Valles Marineris (Witbeck and others, 1991), which is laid out over two sheets and has cross sections; and (3) Olympus Mons (Morris and Tanaka, in press), which has a special map at enlarged scale on a topographic base, text in pamphlet form, cross sections, and extensive figures. In regard to formatting, pay particular attention to the sections on general guidelines, formatting tables, and references cited. (More detailed guidelines for preparing references and a list of examples are given on p. 234–241 of Hansen, 1991.) Careful authors will also study the section on grammar, style, and wording entitled "Suggestions as to Expression" (p. 124–183); this is a misnomer, however, because "suggestions" commonly translates to "orders"! Finally, for the perfectionist who would like to prepare near–camera-ready copy, the Map Coordinator can supply you with a guide to all the formatting instructions used on USGS I–Series maps.

Submittal, Review, and Editing

After your map and accompanying materials have been prepared according to the above guidelines, you must include in your submission (1) the "Manuscript Review and Approval Sheet" (reproduced in Hansen, 1991, p. 38–39), and (2) the "Submission Check List for Planetary Geologic Maps" (Appendix E). The first item, also known as the "route sheet," is used to track USGS products and must accompany them through all prepublication stages. The author completes the top half of the front of the sheet; the Map Coordinator completes the bottom half. An individual's *signature* on the route sheet signifies that the individual is finished with his/her particular processing step. If a person first *initials* the route sheet, he or she is indicating the need for a second review prior to further processing; the author cannot send the map on to the next person named on the route sheet until the previous individual's signature is obtained, unless the Map Coordinator decides otherwise. Although the Chief of the Branch of Astrogeology is required to sign the map at the beginning and end of processing, the Map Coordinator effectively acts as editor–in–charge.

Reviews include a preliminary format review by the Map Coordinator, who will ensure that the submitted materials are in reasonably good order according to the items on the submission check list. Careful attention to these items will greatly speed up the overall review and editing process and will allow technical reviewers to concentrate more on content rather than format. The Coordinator will then pick two technical reviewers (preferably two who are in the VMAP program). Each mapper will be expected to serve as a technical reviewer on two maps. Each review will include a completed "Technical Reviewer's Checklist for Planetary Geologic Maps" (Appendix F). For maps of average or high complexity, a chief reviewer will be assigned who will be required to color the map to assure a thorough review. (Additional suggestions for map reviewers are given by Wilhelms, 1990, p. 257–258, and in Hansen, 1991, p. 230–233.) *When you are given a map to review, it takes priority over your own work!* If an author so requests, the Map Coordinator will advise him/her how to respond to the reviews, particularly for the author's first VMAP map.

Next, the USGS editor will check all material for consistency (internal and external) and for correct English, format, and style. The author will be responsible for producing the revised copies; the final copy, which the drafter will use, is known as the mill copy. It includes the brownline, a neat colored paper copy of the brownline (these two should be consistent), a colored correlation chart, any map overlays, illustration and figure originals, an electronic copy of the map text information on floppy disk, and hard copy of this text. USGS maps require "Author's Check List for Plates, Figures, and Photographs" for each illustration (reproduced in STA7, p. 188–189); these forms serve as work orders for the map drafter. Finally, the author will include a brief abstract (<75 words) for "New Publications of the Geological Survey" (follow *exactly* the format of the example in Hansen, 1991, p. 251).

Finally, the mill copy is submitted for approval by the Director of the USGS. Upon approval, an "I" number is assigned, the map is considered to be "in press," and the Office of Scientific Publications (OSP) of USGS in Flagstaff is given authorization to produce the map. The author or Map Coordinator may be questioned by OSP regarding line work, symbols, layout, unit colors, registration, geographic names, etc. A color proof will eventually be produced for checks by the author, USGS editor, and Map Coordinator.

One last note: a map cannot be cited in a USGS publication until it has been approved by the USGS Director and has an "I" number; if a mapper needs to refer to a colleague's work that has not yet received an "I" number, he/she should write "work in progress in the _____ quadrangle by Doakes (1994) suggests that..." or "map relations in the _____ quadrangle (Doakes, work in progress, 1995) indicate that..." These examples do not appear in Refences Cited, because they are not accessible to the reader.

ACKNOWLEDGMENTS

We particularly wish to thank David Scott (retired USGS) and James Dohm (USGS) for sharing their expertise in coordinating a planetary mapping program and Michael Fienen (formerly USGS) for carrying out various Magellan-based geologic mapping studies of Venus to assist us in determining the challenges that mappers will face. Other useful suggestions and information that have shaped the contents of this handbook were provided by Larry Crumpler (Brown Univ.), Peter Ford (Massachusetts Inst. Tech.), Ron Greeley (Arizona State Univ.), Randy Kirk (USGS), Ted Maxwell (Smithsonian Inst.), Haig Morgan (USGS), Joel Russell (USGS), Jim Underwood (Kansas State Univ.), and Doris Weir (USGS). Funding for the handbook was provided by NASA's Planetary Geology and Geophysics Program.

REFERENCES CITED

Arvidson, R.E., Phillips, R.J., and Izenberg, N., 1992, Global views of Venus from Magellan: Eos, v. 73, p. 161–169.

Batson, R.M., 1990, Cartography, *in* Greeley, Ronald, and Batson, R.M., Planetary Mapping: New York, Cambridge University Press, p. 60–95.

Bindschadler, D.L., Schubert, Gerald, and Kaula, W.M., 1992b, Coldspots and hotspots: Global tectonics and mantle dynamics of Venus: Journal of Geophysical Research, v. 97, no. E8, p. 13,495–13,532.

Burns, B.A., and Campbell, D.B., 1985, Radar evidence for cratering on Venus: Journal of Geophysical Research, v. 90, no. B4, p. 3037-3047.

Campbell, B.A., and Campbell, D.B., 1992, Analysis of volcanic surface morphology on Venus from comparison of Arecibo, Magellan, and terrestrial airborne radar data: Journal of Geophysical Research, v. 97, no. E 10, p. 16,293-16,314.

Campbell, D.B., Head, J.W., Hine, A.A., Harmon, J.K., Senske, D.A., and Fisher, P.C., 1989, Styles of volcanism on Venus: New Arecibo high resolution: Science, v. 246, p. 373-377.

Campbell, D.B., Stacy, N.J.S., and Hine, A.A., 1990, Venus: Crater distribution at low northern latitudes and in the southern hemisphere from new Arecibo observations: Geophysical Research Letters, v. 17, p. 1389-1392.

Campbell, M.H., and Ulrichs, J., 1969, Electrical properties of rocks and their significance for lunar observations: Journal Geophysical Research, v. 74, no. 25, p. 5867-5881.

Dial, A.L., and Schaber, G.G., 1981, Viking orbiter images: Their proper selection for the determination of crater-production rates on geologic units of diverse origins: Third International Colloquium on Mars, p. 62-64.

Dickinson, W.R., Swift, P.N., and Coney, P.J., 1986, Tectonic strip maps of Alpine-Himalayan and Circum-Pacific Orogenic belts: Geological Society of America Map and Chart Series MC-58

Evans, J.V., and Hagfors, T., 1964, On the interpretation of radar reflections from the Moon: Icarus, v. 3, p. 151-160.

Fienen, M.N., Schaber, G.G., and Tanaka, K.L., 1992, Experimental mapping of the V36 quadrangle of Venus, based on Magellan data: Abstracts of papers submitted to the 23rd Lunar and Planetary Science Conference, LPI, Houston, p. 353-354.

Ford, P.G., and G.H. Pettengill, 1992, Venus topography and kilometer–scale slopes: Journal of Geophysical Research, v. 97, no. E8, p. 13,103–13,114.

Ford, J.P., and 8 others, 1989, Spaceborne Radar Observations, A Guide for Magellan Radar–Image Analysis: JPL Publication 89–41, 126 p.

Ford, J.P., and 7 others, 1993, Guide to Magellan Image Interpretation: JPL Publication 93-24, 148 p.

Garvin, J.B., Head, J.W., Pettengill, G.H., and Zisk, S.H., 1985, Venus global radar-reflectivity and correlations with elevation: Journal Geophysical Research, v. 90, no. 88, p. 6859-6871.

Greeley, Ronald, and 10 others, 1992, Aeolian features on Venus: Preliminary Magellan results: Journal of Geophysical Research, v. 97, no. E8, p. 13,319–13,346.

Hagfors, T., 1964, Backscattering from an undulating surface with application to radar returns from the Moon: Journal of Geophysical Research, v. 69, pp. 3779-3784.

Hansen, W.R. (ed.), 1991, Suggestions to Authors of the Reports of the United States Geological Survey, 7th ed.: Washington, D.C., U.S. Government Printing Office, 289 p.

Head, J.W., and 7 others, 1991, Venus volcanism: Initial analysis from Magellan data: Science, v. 252, p. 276–288.

Head, J.W., Crumpler, L.S., Aubele, J.C., Guest, J.E., and Saunders, R.S., 1992, Venus volcanism: Classification of volcanic features and structures, associations, and global distribution from Magellan Data: Journal of Geophysical Research, v. 97, no. E8, p. 13,153–13,198.

Howell, D.G., ed., 1985, Tectonostratigraphic Terranes of the Circum-Pacific Region: Circum-Pacific Council for Energy and Mineral Resources, Houston, 581p.

Izenberg, N.R., 1992, Venusian extended ejecta deposits as time-stratigraphic markers: *in* Papers presented to the International Colloquium on Venus, Pasadena, Calif., August 10–12, 1992, LPI Contribution No. 789, p. 49-50.

Jurgens, R.F., Goldstein, R.M., Rumsey, H.R., and Green, R.R., 1980, Images of Venus by three-station interferometry: 1977 results: Journal of Geophysical Research, v. 85, p. 8282-8294.

Jurgens, R.F., and 8 others, 1988a, High resolution images of Venus from ground-based radar: Geophysical Research Letters, v. 15, p. 577-580.

Jurgens, R.F., Slade, M.A., and Saunders, R.S., 1988b, Evidence for highly reflective materials on the surface and subsurface of Venus: Science, v. 240, p. 1021-1023.

King, P.B., compiler, 1969a, Tectonic Map of North America: U.S. Geological Survey, scale 1:5,000,000.

King, P.B., 1969b, The tectonics of North America--A discussion to accompany the tectonic map of North America, scale 1:5,000,000: U.S. Geological Survey Professional Paper 628, 95p.

King, P.B., and Edmonston, G.J., 1972, Generalized tectonic map of North America: U.S. Geological Survey Miscellaneous Investigations Series Map I-688.

Kirk, R.L., Soderblom, L. A., and Lee, E.M., 1992, Enhanced visualization for interpretation of Magellan radar data: Supplement to the Magellan special issue: Journal of Geophysical Research, v. 97, no. E10, p. 16,371-16,380.

Klose, K.B., Wood, J.A., and Hashimoto, A., 1992, Mineral equilibria and the high radar reflectivity of Venus mountain tops: Journal of Geophysical Research, v. 97, no. E10, p. 16,353-16,370.

Kotelnikov, B.A. (ed.), 1989, Atlas of the Surface of Venus: Moscow, Main Directorate of Geodesy and Cartography, 328p.)

Leberl, F.W., Thomas, J.K., and Maurice, K.E., 1992, Initial results from the Magellan stereo experiment: Journal of Geophysical Research, v. 97, no. E8, p. 13,675–13,689.

Masursky, Harold, Eliason, Eric, Ford, P.G., McGill, G.E., Pettengill, G.H., Schaber, G.G., and Schubert, Gerald, 1980, Pioneer Venus radar results: Geology from images and altimetry: Journal of Geophysical Research, v. 85, no. A13, p. 8232-8260.

Michaels, Greg, 1992, Magellan guide for the interpretation of synthetic aperture radar images: JPL D–9756, Pasadena, Calif., Jet Propulsion Laboratory, 3 tables and 19 figures.

Milton, D.J., 1975, Geologic map of the Lunae Palus quadrangle of Mars: U.S. Geological Survey Miscellaneous Investigations Series Map I–894, scale 1:5,000,000.

Moore, H.J., and Thompson, T.W., 1988, Crater identification and resolution of lunar radar images: Proceedings 18th Lunar and Planetary Science Conference, p. 383-395.

Moore, H.J., Boyce, J.M., Schaber, G.G., and Scott, D.H., 1980, Lunar remote sensing and measurements: U.S. Geological Survey Professional Paper 1046-B, 78p.

Moore, H.J., Plaut, J.J., Schenk, P.M., and Head, J.W., 1992, An unusual volcano on Venus: Journal of Geophysical Research, v. 97, no. E8, p. 13,479–13,494.

Moore, H.J., Plaut, J.J., and Parker, T.J., 1993, Relief of some small landforms on Venus (abstract): Lunar and Planetary Science Conference XXIV, p. 1003-1004.

Moore, H.J., Tyler, G.L., Boyce, J.M., Shorthill, R.W., Thompson, T.W., Wilhelms, D.E., Wu, S.S.C., and Zisk, S.H., 1976, Correlation of photogeology and remote sensing data along the Apollo 14, 15, and 16 bistatic-radar ground tracks, Part II--a working compendium: U.S. Geological Survey Open-File Report 76-298, 101p.

Morris, E.C., and Tanaka, K.L., in press, Geologic maps of the Olympus Mons region of Mars: U.S. Geological Survey Miscellaneous Investigations Series Map I–2327, scales 1:2,000,000 and 1:1,000,000.

Muhleman, D.O., 1964, Radar scattering from the Moon and Venus: Astronomical Journal, v. 69, p. 34041.

North American Commission on Stratigraphic Nomenclature, 1983, North American stratigraphic code: American Association of Petroleum Geologists Bulletin, v. 67, no. 5, p. 841–875.

Olhoeft, G.R., and Strangway, D.W., 1975, Dielectric properties of the first 100 meters of the Moon: Earth and Planetary Science Letters, v. 24, p. 394-404.

Pettengill, G.H., Ford, P.G., and Chapman, B.D., 1988, Venus surface electrical properties: Journal Geophysical Research, v. 93, p. 14,881-14,892.

Pettengill, G.H., Ford, P.G., Johnson, W.T.K., Raney, R.K., and Soderblom, L.A., 1991, Magellan: Radar performance and data products: Science, v. 252, p. 260–265.

Pettengill, G.H., Ford, P.G., and Wilt, R.J., 1992, Venus surface radiothermal emission as observed by Magellan: Journal of Geophysical Research, v. 97, no. E8, p. 13,091–13,102.

Phillips, R.J., Raubertas, R.F., Arvisdon, R.E., Sarkar, I.C., Herrick, R.R., Izenberg, Noam, and Grimm, R.E., 1992, Impact craters and Venus resurfcaing history: Journal of Geophysical Research, v. 97, no. E10, p. 15,923-15,948.

Plaut, J.J., 1991, Radar scattering as a source of geologic information on Venus and Earth: PhD thesis, Washington University, St. Louis, 342p.

Plaut, J.J., 1993, Magellan stereo image data: V-Gram (Magellan Bulletin about Venus and the Radar Mapping Mission) Jet Propulsion Laboratory, Pasadena, CA, April 1993, p. 14-18.

Plaut, J.J., and Arvidson, R.E., 1992, Comparison of Goldstone and Magellan radar data in the equatorial plains of Venus: Journal of Geophysical Research, v. 97, no. E10, p. 16,279-16,292.

Plaut, J.J., and 11 others, 1992, Anomalous scattering behavior of selected impact "parabolic" features: Magellan cycle-to-cycle comparisons: *in* Papers presented to the International Colloquium on Venus, August 10-12, 1992, Pasadena, Calif., LPI Contribution No. 789, p. 92-93.

Reynolds, M.W., Queen, J.E., Ratcliffe, N.M., Escowitz, E.C., Taylor, R.B., Davis, J.B., and Scott, W.E., in press, Cartographic and digital standards for earth science publications—principles, symbols, colors, patterns, codes, and formats: U.S. Geological Survey Open–File Report 90–0001.

Saint-Amant, M., and Strangway, D.W., 1970, Dielectric properties of dry, geologic materials: Geophysics, v. 35, no. 4, p. 624-645.

Saunders, R.S., and Pettengill, G.H., 1991, Magellan: Mission summary: Science, v. 252, p. 247–249.

Saunders, R.S., Pettengill, G.H., Arvidson, R.E., Sjogren, W.L., Johnson, W.T.K., and Pieri, L., 1990, The Magellan Venus Radar Mapping Mission: Journal of Geophysical Research, v. 95, p. 8339–8355.

Saunders, R.S., and 26 others, 1992, Magellan Mission summary: Journal of Geophysical Research, v. 97, no. E8, p. 13,067–13,090.

Schaber, G.G., 1990, Venus: Quantitative analyses of terrain units identified from Venera 15/16 data and described in open-file report 90-24: U.S. Geological Survey Open-File Report 90-468, 25 p., 34 figs.

Schaber, G.G., and Kozak, R.C., 1990, Geologic/Geomorphic and Structure Maps of the Northern Quarter of Venus: U.S. Geologic Survey Open–File Report 90–24, 1:15,000,000 scale.

Schaber, G.G., and 9 others, 1992, Geology and distribution of impact craters on Venus: What are they telling us?: Journal of Geophysical Research, v. 97, No. E8, pp. 13,257-13,301.

Schmugge, Thomas, 1980, Techniques and applications of microwave radiometry: *in* Siegel, B.S., and Gillespie, A.R., eds, Remote Sensing in Geology, John Wiley and Sons, New York, p. 337-361.

Scott, D.H., and Tanaka, K.L., 1986, Geologic map of the western equatorial region of Mars: U.S. Geological Survey Miscellaneous Investigations Series Map I–1802–A, scale 1:15,000,000.

Senske, D.A., Schaber, G.G., and Stofan, E.R., 1992, Regional topographic rises on Venus: Geology of Western Eistla Regio and comparison to Beta Regio and Atla Regio: Journal of Geophysical Research, v. 97, no. E8, p. 13,395–13,420.

Solomon, S.C. and 7 others, 1991, Venus tectonics: Initial analysis from Magellan: Science, v. 252, p. 297–312.

Solomon, S.C. and 10 others, 1992, Venus tectonics: An overview of Magellan observations: Journal of Geophysical Research, v. 97, no. E8, p. 13,199–13,256.

Squyres, S.W., Janes, D.M., and 5 others, 1992a, The morphology and evolution of coronae on Venus: Journal of Geophysical Research, v. 97, no. E8, p. 13,611–13,634.

Stofan, E.R., and 7 others, 1992, Global distribution and characteristics of coronae and related features on Venus: Implications for origin and relation to mantle processes: Journal of Geophysical Research, v. 97, no. E8, p. 13,347–13,378.

Sukhanov, A.L. and 11 others, 1989, Geomorphic/geologic map of part of the northern hemisphere of Venus: U.S. Geological Survey Miscellaneous Investigations Series Map I–2059, scale 1:15,000,000.

Tanaka, K.L., and Schaber, G.G., 1992, Can a time–stratigraphic system be developed for Venus?: *in* Papers presented to the International Colloquium on Venus, Pasadena, Calif., August 10–12, 1992, LPI Contribution No. 789, p. 20–21.

Tyler, G.L., Ford, P.G., Campbell, D.B., Elachi, C., Pettengill, G.H., and Simpson, R.A., 1991, Magellan: Electrical and physical properties of Venus' surface: Science, v. 252, p. 265–270.

Tyler, G.L., Simpson, R.A., Maurer, M.J., and Edgar Holmann, 1992, Scattering properties of the Venusian surface: Preliminary results from Magellan: Journal of Geophysical Research, v. 97, no. E8, p. 13,115–13,140.

Weitz, C.M., Moore, H.J., and Schaber, G.G., 1992, Low-emissivity impact craters on Venus: *in* Abstracts submitted to the Twenty-Third Lunar and Planetary Science Conference, part 3, p. 1513-1514.

Wilhelms, D.E., 1990, Geologic mapping, *in* Greeley, Ronald, and Batson, R.M., Planetary Mapping: New York, Cambridge University Press, p. 208–260.

Wise, D.U., 1969, Pseudo-radar topographic shadowing for detection of sub-continental sized fracture systems: *in* Proceedings of the Sixth International Symposium on Remote Sensing of Environment, Ann Arbor, p. 603-615.

Witbeck, N.E., Tanaka, K.L., and Scott, D.H., 1991, Geologic map of the Valles Marineris region, Mars: U.S. Geological Survey Miscellaneous Investigations Series Map I–2010, scale 1:2,000,000.

Yamaguchi, Y., 1985, Image-scale and look-direction effects on the detectability of lineaments in radar images: Remote Sensing of Environment, v. 17, p. 117-127.

Young, Carolynn (ed.), 1990, The Magellan Venus Explorer's Guide: JPL Publication 90-24, 197 p., topographic map insert.

RECOMMENDED READING

The following topical lists provide comprehensive references pertinent to geologic mapping of Venus. Particularly note three special journal issues describing the Magellan mission and data and preliminary science results:

"Magellan At Venus," 1991, Science, v. 252, p. 181-344.
"Magellan At Venus," 1992, Journal of Geophysical Research, v. 97, nos. E8 and E10.

Geologic Mapping: Philosophy, Style, and Conventions

Batson, R.M., 1990, Cartography, *in* Greeley, Ronald, and Batson, R.M., Planetary Mapping: New York, Cambridge University Press, p. 60–95.

Fienen, M.N., Schaber, G.G., and Tanaka, K.L., 1992, Experimental mapping of the V36 quadrangle of Venus, based on Magellan data: Abstracts of papers submitted to the 23rd Lunar and Planetary Science Conference, LPI, Houston, p. 353-354.

Hansen, W.R. (ed.), 1991, Suggestions to Authors of the Reports of the United States Geological Survey, 7th ed.: Washington, D.C., U.S. Government Printing Office, 289 p.

Harrison, J.M., 1963, Nature and significance of geological maps, *in* Albritton, C.C., The Fabric of Geology: San Francisco, Freeman, p. 225–232.

Irvine, T.N., Rumble, Douglas, and Irvine, L.M., 1992, A writing guide for petrological (and other geological) manuscripts: Journal of Petrology, 46 p.

Milton, D.J., 1975, Geologic map of the Lunae Palus quadrangle of Mars: U.S. Geological Survey Miscellaneous Investigations Series Map I–894, scale 1:5,000,000.

Morris, E.C., and Tanaka, K.L., in press, Geologic maps of the Olympus Mons region of Mars: U.S. Geological Survey Miscellaneous Investigations Series Map I–2327, scales 1:2,000,000 and 1:1,000,000.

North American Commission on Stratigraphic Nomenclature, 1983, North American stratigraphic code: American Association of Petroleum Geologists Bulletin, v. 67, no. 5, p. 841–875.

Reynolds, M.W., Queen, J.E., Ratcliffe, N.M., Escowitz, E.C., Taylor, R.B., Davis, J.B., and Scott, W.E., in press, Cartographic and digital standards for earth science publications—principles, symbols, colors, patterns, codes, and formats: U.S. Geological Survey Open-File Report 90–0001.

Sandwell, D.T., and Schubert, Gerald, 1992, Flexural ridges, trenches, and outer rises around coronae on Venus: Journal of Geophysical Research, v. 97, no. E10, p. 16,069-16,084.

Schaber, G.G., 1990, Venus: Quantitative analyses of terrain units identified from Venera 15/16 data and described in open-file report 90-24: U.S. Geological Survey Open-File Report 90-468, 25 p., 34 figs.

Schaber, G.G., and Kozak, R.C., 1990, Geologic/Geomorphic and Structure Maps of the Northern Quarter of Venus: U.S. Geologic Survey Open–File Report 90–24, 1:15,000,000 scale.

Scott, D.H., and Tanaka, K.L., 1986, Geologic map of the western equatorial region of Mars: U.S. Geological Survey Miscellaneous Investigations Series Map I–1802–A, scale 1:15,000,000.

Sukhanov, A.L., and 11 others, 1989, Geomorphic/geologic map of part of the northern hemisphere of Venus: U.S. Geological Survey Miscellaneous Investigations Series Map I–2059, scale 1:15,000,000.

Tanaka, K.L., and Schaber, G.G., 1992, Can a time–stratigraphic system be developed for Venus?: *in* Papers presented to the International Colloquium on Venus, Pasadena, Calif., August 10–12, 1992, LPI Contribution No. 789, p. 20–21.

Wilhelms, D.E., 1990, Geologic mapping, *in* Greeley, Ronald, and Batson, R.M., Planetary Mapping: New York, Cambridge University Press, p. 208–260.

Witbeck, N.E., Tanaka, K.L., and Scott, D.H., 1991, Geologic map of the Valles Marineris region, Mars: U.S. Geological Survey Miscellaneous Investigations Series Map I–2010, scale 1:2,000,000.

Overviews of Magellan Mission, Sensors, and Data Products

Johnson, W.T.K., 1991, Magellan imaging radar mission to Venus: IEEE Proc., v. 79, pp. 777-790.

Pettengill, G.H., Ford, P.G., Johnson, W.T.K., Raney, R.K., and L.A. Soderblom, 1991, Magellan: Radar performance and data products: Science, v. 252, pp. 260-265.

Saunders, R.S., Pettengill, G.H., Arvidson, R.E., Sjogren, W.L., Johnson, W.T.K., and Pieri, L., 1990, The Magellan Venus Radar Mapping Mission: Journal of Geophysical Research, v. 95, p. 8339–8355.

Saunders, R.S., and 26 others, 1992, Magellan Mission summary: Journal of Geophysical Research, v. 97, no. E8, p. 13,067–13,090.

Young, Carolynn (ed.), 1990, The Magellan Venus Explorer's Guide: JPL Publication 90-24, 197 p., topographic map insert.

General Geology and Topography of Venus

Basilevsky, A.T., and Head, J.W., 1988, The geology of Venus: Annual Reviews of Earth and Planetary Science, v. 16, p. 295-317.

Leberl, F.W., Maurice, K.E., Thomas, J.K., Leff, C.E., and Wall, S.D., 1992, Images and topographic relief at the north pole of Venus: Journal of Geophysical Research, v. 97, no. E8, p. 13,667-13,674.

Leberl, F.W., Thomas, J.K., and Maurice, K.E., 1992, Initial results from the Magellan stereo experiment: Journal of Geophysical Research, v. 97, no. E8, p. 13,675-13,689.

Saunders, R.S., Arvidson, R.E., Head, J.W. III, Schaber, G.G., Stofan, E.R., and Soloman, S.C., 1991, An overview of Venus geology: Science, v. 252, p. 249–251.

Saunders, R.S., and Stofan, E.R., 1991, Magellan: Progress on a global geologic reconnaissance map of Venus: Geological Society of America Abstracts with Programs, 1991 Annual Meeting, San Diego, California, p. A399–A400.

Schaber, G.G., 1990, Venus: Quantitative analyses of terrain units identified from Venera 15/16 data and described in open-file report 90-24: U.S. Geological Survey Open-File Report 90-468, 25 p., 34 figs.

Solomon, S.C., and Head, J.W., 1991, Fundamental issues in the geology and geophysics of Venus: Science, v. 252, p. 252-260.

Sukhanov, A.L., and 11 others, 1989, Geomorphic/geologic map of part of the northern hemisphere of Venus: U.S. Geological Survey Miscellaneous Investigations Series Map I–2059, scale 1:15,000,000.

Tanaka, K.L., and Schaber, G.G., 1992, Can a time–stratigraphic system be developed for Venus?: *in* Papers presented to the International Colloquium on Venus, Pasadena, Calif., August 10–12, 1992, LPI Contribution No. 789, p. 20–21.

Impact Craters and Resurfacing History of Venus

Arvidson, R.E., Grimm, R.E., Phillips, R.J., Schaber, G.G., and Shoemaker, E.M., 1991, On the nature and rate of resurfacing of Venus: Geophysical Research Letters, v. 17, p. 1385-1388.

Asimow, P.D., and Wood, J.A., 1992, Fluid outflows from Venus impact craters: Analysis from Magellan data: Journal of Geophysical Research, v. 97, no. E8, p. 13,643–13,666.

Basilevsky, A.T., and 7 others, 1987, Impact craters on Venus: A continuation of the analysis of data from the Venera 15 and 16 spacecraft: Journal of Geophysical Research, v. 92, p. 12,869-12,901.

Campbell, D.B., and 7 others, 1992, Magellan observations of extended impact crater related features on the surface of Venus: Journal of Geophysical Research, v. 97, no. E10, p. 16,249-16,278.

Ivanov, B.A., 1990, Venusian impact craters of Magellan images: View from Venera 15/16: Earth, Moon, and Planets, v. 50/51, p. 159-173.

Ivanov, B.A., and Basilevsky, A.T., 1987, A comparison of crater retention ages on the Earth and Venus: Solar System Research, v. 21, p. 84-89.

Ivanov, B.A., Basilevsky, A.T., Kryuchkov, V.P., and Chernaya, I.M., 1986, Impact craters on Venus: Analysis of Venera 15 and 16 data: Proceedings Lunar and Planetary Science Conference, 16th, part 2, Journal of Geophysical Research, v. 91, suppl., p. D414-D430.

Ivanov, B.A., Nemchinov, I.V., Svetsov, V.A., Provalov, A.A., Khazins, V.M., and Phillips, R.J., 1992, Impact cratering on Venus: Physical and mechanical models: Journal of Geophysical Research, v. 97, no. E10, p. 16,167-16,182.

Melosh, H.J., 1989, Impact cratering—A geologic process: Oxford Monographs on Geology and Geophysics No. 11, New York, Oxford University Press, 245 p.

Phillips, R.J., Arvidson, R.E., Boyce, J.M., Campbell, D.B., Guest, J.E., Schaber, G.G., and Soderblom, L.A., 1991, Impact craters on Venus: Initial analysis from Magellan data: Science, v. 252, p. 288–296.

Phillips, R.J., Raubertas, R.F., Arvidson, R.E., Sarkar, I.C., Herrick, R.R., Izenberg, Noam, and Grimm, R.E. 1992, Impact craters and Venus resurfacing history: Journal of Geophysical, no. E10, p. 15,923-15,948.

Schaber, G.G., Shoemaker, E.M., and Kozak, R.C., 1987, The surface age of Venus: Use of the terrestrial cratering record (in Russian): Astronomicheskiiy Vestnik, v. 21, p. 144-150. (Also in English: Solar System Research, v. 21, p. 89-94, 1987)

Schaber, G.G., and 9 others, Geology and distribution of impact craters on Venus: What are they telling us?: Journal of Geophysical Research, v. 97, no. E8, p. 13,257-13,302.

Schultz, P.H., 1992, Atmospheric effects on ejecta emplacement and crater formation on Venus from Magellan: Journal of Geophysical Research, v. 97, no. E10, p. 16,183-16,248.

Volcanism on Venus

Baker, V.R., Komatsu, Goro, Parker, T.J., Gulick, V.C., Kargel, J.S., and Lewis, J.S., 1992, Channels and valleys on Venus: Preliminary analysis of Magellan data: Journal of Geophysical Research, v. 97, no. E8, p. 13,421–13,444.

Campbell, B.A., and Campbell, D.B., 1992, Analysis of volcanic surface morphology on Venus from comparison of Arecibo, Magellan, and terrestrial airborne radar data: Journal of Geophysical Research, v. 97, no. E10, p. 16,293-16,314.

Guest, J.E., and 8 others, 1992, Small volcanic edifices and volcanism in the plains of Venus: Journal of Geophysical Research, v. 97, no. E10, p. 15,949-15,966.

Head, J.W., and 7 others, 1991, Venus volcanism: Initial analysis from Magellan data: Science, v. 252, p. 276–288.

Head, J.W., Crumpler, L.S., Aubele, J.C., Guest, J.E., and Saunders, R.S., 1992, Venus volcanism: Classification of volcanic features and structures, associations, and global distribution from Magellan Data: Journal of Geophysical Research, v. 97, no. E8, p. 13,153–13,198.

McKenzie, Dan, Ford, P.G., Liu, Fang, and Pettengill, G.H., 1992, Pancakelike domes on Venus: Journal of Geophysical Research, v. 97, no. E10, p. 15,967-15,976.

McKenzie, D., McKenzie, J.M., and Saunders, R.S., 1992, Dike emplacement on Venus and on Earth: Journal of Geophysical Research, v. 97, no. E8, p. 15,977-15,990.

Moore, H.J., Plaut, J.J., Schenk, P.M., and Head, J.W., 1992, An unusual volcano on Venus: Journal of Geophysical Research, v. 97, no. E8, p. 13,479–13,494.

Pavri, Betina, Head, J.W., Klose, K.B., and Wilson, Lionel, 1992, Steep-sided domes on Venus: Characteristics, geologic setting, and eruption conditions from Magellan data: Journal of Geophysical Research, v. 97, no. E8, p. 13,445–13,478.

Roberts, K.M., Guest, J.E., Head, J.W., and Lancaster, M.G., 1992, Mylitta Fluctus, Venus: Rift-related, centralized volcanism and the emplacement of large-volume flow units: Journal of Geophysical Research, v. 97, no. E10, p. 15,991-16,016.

Senske, D.A., Schaber, G.G., and Stofan, E.R., 1992, Regional topographic rises on Venus: Geology of Western Eistla Regio and comparison to Beta Regio and Atla Regio: Journal of Geophysical Research, v. 97, no. E8, p. 13,395–13,420.

Structure, Tectonism, and Geophysics on Venus

Ananda, M.P., Sjogren, W.L., Phillips, R.J., Wimberly, R.N., and Bills, B.G., 1980, A low-order global gravity field of Venus and dynamical implications: Journal of Geophysical Research, v. 85, no. A13, p. 8303-8318.

Banerdt, W.B., 1986, Support of long-wavelength loads on Venus and implications for internal structure: Journal of Geophysical Research, v. 91, no. B1, p. 403-419.

Banerdt, W.B., and Golombek, M.P., 1988, Deformational models of rifting and folding on Venus: Journal of Geophysical Research, v. 93, p. 4759-4772.

Banerdt, W.B., and Sammis, C.G., 1992, Small-scale fracture patterns on the volcanic plains of Venus: Journal of Geophysical Research, v. 97, no. E10, p. 16,149-16,166.

Bills, B.G., Kiefer, W.S., and Jones, R.L., 1987, Venus gravity: A harmonic analysis: Journal of Geophysical Research, v. 92, no. B10, p. 10,335-10,351.

Bills, B.G., and Kobrick, M., 1985, Venus topography: A harmonic analysis: Journal of Geophysical Research, v. 90, no. B1, p. 827-836.

Bindschadler, D.L., and Parmentier, E.M., in press, Mantle flow tectonics: The influence of a ductile lower crust and implications for the formation of topographic uplands on Venus: Journal of Geophysical Research.

Bindschadler, D.L., deCharon, Annette, Beratan, K.K., Smrekar, S.E., and Head, J.W., 1992a, Magellan observations of Alpha Regio: Implications for formation of complex ridged terrains on Venus: Journal of Geophysical Research, v. 97, no. E8, p. 13,563–13,578.

Bindschadler, D.L., Schubert, Gerald, and Kaula, W.M., 1990, Mantle flow tectonics and the origin of Ishtar Terra, Venus: Geophysical Research Letters, v. 17, p. 1345-1348.

Bindschadler, D.L., Schubert, Gerald, and Kaula, W.M., 1992b, Coldspots and hotspots: Global tectonics and mantle dynamics of Venus: Journal of Geophysical Research, v. 97, no. E8, p. 13,495–13,532.

Grimm, R.E., and Phillips, R.J., 1992, Anatomy of a Venusian hot spot: Geology, gravity, and mantle dynamics of Eistla Regio: Journal of Geophysical Research, v. 97, no. E10, p. 16,035-16,054.

Herrick, R.H., and Phillips, R.J., 1992, Geological correlations with the interior density structure of Venus: Journal of Geophysical Research, v. 97, no. E10, p. 16,017-16,034.

Janes, D.M., Squyres, S.W., Bindschadler, D.L., Baer, Gidon, Schubert, Gerald, Sharpton, V.L., and Stofan, E.R., 1992, Geophysical models for the formation and evolution of coronae on Venus: Journal of Geophysical Research, v. 97, no. E10, p. 16,055-16,068.

Johnson, C.L., and Sandwell, D.T., 1992, Joints in Venusian lava flows: Journal of Geophysical Research, v. 97, no. E8, p. 13,601–13,610.

Kaula, W.M., 1990, Venus: A contrast in evolution to Earth: Science, v. 247, p. 1191-1196.

Kaula, W.M., 1990, Mantle convection and crustal evolution on Venus: Geophysical Research Letters, v. 17, p. 1401.

Kaula, W.M., Bindschadler, D.L., Grimm, R.E., Hansen, V.L., Roberts, K.M., and Smrekar, S.E., 1992, Styles of deformation in Ishtar Terra and their implications: Journal of Geophysical Research, v. 97, no. E10, p. 16,085-16,121.

McKenzie, Dan, Ford, P.G., Johnson, Catherine, Parsons, Barry, Sandwell, D.T., Saunders, R.S., and Solomon, S.C., 1992, Features on Venus generated by plate boundary processes: Journal of Geophysical Research, v. 97, no. E8, p. 13,533–13,544.

Phillips, R.J., Grimm, R.E., and Malin, M.C., 1991, Hot-spot evolution and the global tectonics of Venus: Science, v. 252, p. 651-658.

Sandwell, D.T., and Schubert, Gerald, 1992, Flexural ridges, trenches, and outer rises around coronae on Venus: Journal of Geophysical Research, v. 97, no. E10, p. 16,069-16,084.

Smrekar, S.E., and Solomon, S.C., 1992, Gravitational spreading of high terrain in Ishtar Terra, Venus: Journal of Geophysical Research, v. 97, no. E10, p. 16,121-16,148.

Solomon, S.C., and Head, J.W., 1991, Fundamental issues in the geology and geophysics of Venus: Science, v. 252, p. 252–260.

Solomon, S.C., and 7 others, 1991, Venus tectonics: Initial analysis from Magellan: Science, v. 252, p. 297–312.
Solomon, S.C., and 10 others, 1992, Venus tectonics: An overview of Magellan observations: Journal of Geophysical Research, v. 97, no. E8, p. 13,199–13,256.
Squyres, S.W., Janes, D.M., Baer, Gidon, Bindschadler, D.B., Schubert, Gerald, Sharpton, V.L., and Stofan, E.R., 1992a, The morphology and evolution of coronae on Venus: Journal of Geophysical Research, v. 97, no. E8, p. 13,611–13,634.
Stofan, E.R., Sharpton, V.L., Schubert, Gerald, Baer, Gidon, Bindschadler, D.L., Janes, D.M., and Squyres, S.W., 1992, Global distribution and characteristics of coronae and related features on Venus: Implications for origin and relation to mantle processes: Journal of Geophysical Research, v. 97, no. E8, p. 13,347–13,378.
Squyres, S.W., Jankowski, D.G., Simons, Mark, Solomon, S.C., Hagar, B.H., and McGill, G.E., 1992b, Plains tectonism on Venus: The deformation belts of Lavinia Planitia: Journal of Geophysical Research, v. 97, no. E8, p. 13,579–13,600.
Suppe, John, and Connors, Chris, 1992, Critical taper wedge mechanics of fold–and–thrust belts on Venus: Initial results from Magellan: Journal of Geophysical Research, v. 97, no. E8, p. 13,545–13,562.
Vorder Bruegge, R.W., and Head, J.W., 1989, Fortuna Tessera, Venus: Evidence of horizontal convergence and crustal thickening: Geophysical Research Letters, v. 16, p.699-702.
Zuber, M.T., 1987, Constraints on the lithospheric structure of Venus from mechanical models and tectonic surface features: Journal of Geophysical Research, v. 92, no. B4, p. E541-E551.
Zuber, M.T., 1990, Ridge Belts: Evidence for regional- and local-scale deformation on the surface of Venus: Geophysical Research Letters, v. 17, p. 1369-1372.

Surface Properties and Modification on Venus

Arvidson, R.E., V.R. Baker, C. Elachi, R.S. Saunders, and J.A. Wood, 1991, Magellan: Initial analysis of Venus surface modification: Science, v. 252, p. 270–275.
Arvidson, R.E., and 7 others, 1992, Surface modification of Venus as inferred from Magellan observations of plains: Journal of Geophysical Research, v. 97, no. E8, p. 13,303–13,318.
Greeley, Ronald, and Marshall, J.R., 1985, Transport of Venusian rolling 'stones' by wind: Nature, v. 313, p. 771-773.
Greeley, Ronald, Marshall, J.R., and Leach, R.N., 1984, Microdunes and other aeolian bedforms on Venus: Wind tunnel simulations: Icarus, v. 60, p. 152-160.
Greeley, Ronald, Marshall, J.R., and Pollack, J.B., 1987, Venus: Physical and chemical modification of the surface by windblown particles: Nature, v. 327, p. 313-315.
Greeley, Ronald, and 10 others, 1992, Aeolian features on Venus: Preliminary Magellan results: Journal of Geophysical Research, v. 97, no. E8, p. 13,319–13,346.
Klose, K.B., Wood, J.A., and Hashimoto, A., 1992, Mineral equilibria and the high radar reflectivity of Venus mountain tops: Journal of Geophysical Research, v. 97, no. E10, p. 16,353-16,370.
Malin, M.C., 1992, Mass movements on Venus: Preliminary results from Magellan cycle 1 observations: Journal of Geophysical Research, v. 97, no. E10, p. 16,337-16,352.
Marshall, J.R., Greeley, Ronald, and Tucker, D.W., 1988, Aeolian weathering of Venusian surface materials: Preliminary results from laboratory simulations: Icarus, v. 74, p. 495-515.
Pettengill, G.H., Ford, P.G., and Wilt, R.J., 1992, Venus surface radiothermal emission as observed by Magellan: Journal of Geophysical Research, v. 97, no. E8, p. 13,091-13,102.
Tyler, G.L., Ford, P.G., Campbell, D.B., Elachi, Charles, Pettengill, G.H., and Simpson, R.A., 1991, Magellan: Electrical and physical properties of Venus: Science, v. 252, p. 265-270.
Tyler, G.L., Simpson, R.A., Maurer, M.J., and Holmann, Edgar, 1992, Scattering properties of the Venusian surface: preliminary results from Magellan: Journal of Geophysical Research, v. 97, no. E8, p. 13,115-13,139.
Tryka, K.A., and Muhleman, D.O., 1992, Reflection and emission properties on Venus: Alpha Regio: Journal of Geophysical Research, v. 97, no. E8, p. 13, 379–13,394.

Non-Magellan Radar and Other Data

Earth-based results

Arvidson, R.E., Plaut, J.J., Jurgens, R.F., Saunders, R.S., and Slade, M.A., 1990, Geology of southern Guinevere Planitia, Venus based on analysis of Goldstone radar data: Proceedings Lunar and Planetary Science Conference, 20th, p. 557-572.

Campbell, D.B., and Burns, B.A., 1980, Earth-based radar imagery of Venus: Journal of Geophysical Research, v. 85, no. A13, p. 8271-8281.

Campbell, D.B., Head, J.W., Hine, A.A., Harmon, J.K., Senske, D.A., and Fisher, P.C., 1989, Styles of volcanism on Venus: New Arecibo high resolution radar data: Science, v. 246, p. 373-377.

Goldstein, R.M., Green, R.R., and Rumsey, H.C., 1976, Venus radar images: Journal of Geophysical Research, v. 81, p. 4807-4817.

_______1978, Venus radar brightness and altitude images: Icarus, v. 36, p. 334-362.

Jurgens, R.F., Goldstein, R.M., Rumsey, H.R., and Green, R.R., 1980, Images of Venus by three-station radar interferometry - 1977 results: Journal of Geophysical Research, v. 85, no. A13, p. 8282-8294.

Jurgens, R.F., Slade, M.A., and Saunders, R.S., 1988, Evidence for highly reflecting materials on the surface and subsurface of Venus: Science, v. 240, p. 1021-1023.

Jurgens, R.F., and 8 others, 1988, High resolution images of Venus from ground-based radar: Geophysical Research Letters, v. 15, p. 577-580.

Plaut, J.J., Arvidson, R.E., and Jurgens, R.F., 1990, Radar characteristics of the equatorial plains of Venus from Goldstone Observations: Implications to interpretation of Magellan data: Geophysical Research Letters, v. 17, p. 1357-1360.

Venera and Vega overviews

Barsukov, V.L., and Basilevsky, A.T., 1986, The Geology of Venus, *translation of* "Geologiya Venery", Priroda, v. 6: *in* NASA TM-88567, p. 24-35.

Barsukov, V.L., and 29 others, 1986, The geology and geomorphology of the Venus surface as revealed by the radar images obtained by Veneras 15 and 16: Journal of Geophysical Research, v. 91, p. D378-D398.

Basilevsky, A.T., Nikolaeva, O.V., and Weitz, C.M., 1992, Geology of the Venera 8 landing site region from Magellan data: Morphological and geochemical considerations, Journal of Geophysical Research, v. 97, no. E10, p. 16,315-16,335.

Basilevsky, A.T., Pronin, A.A., Ronca, L.B., Kryuchkov, V.P., and Sukhanov, A.L., 1986, Styles of tectonic deformations on Venus: Analysis of Venera 15 and 16 data: Proceedings Lunar and Planetary Science Conference, 16th, part 2, Journal of Geophysical Research, v. 91, suppl., p. D399-D411.

Bindschadler, D.L., Head, J.W., and Garvin, J.B., 1986, Vega landing sites: Venera 15/16 unit analogs from Pioneer Venus reflectivity and RMS slope data: Geophysical Research Letters, v. 13, p. 1415-1418.

Kotelnikov, V.A., Bogomolov, A.F., and Rzhiga, O.N., 1985, Radar study of Venus surface by Venera-15 and -16 spacecraft: Advances in Space Research, v. 5, p. 2-16.

See also:

"Geology and Tectonics of Venus," Earth, Moon, and Planets, 1990, v. 50/51, p. 3-578.

Earth, Moon, and Planets, 1990, v. 55, no. 2, p. 97-214.

Pioneer Venus results

Bindschadler, D.L., and Head, J.W., 1989, Characterization of Venera 15/16 geologic units from Pioneer Venus reflectivity and roughness data: Icarus, v. 77, p. 3-20.
Davis, P.A., Kozak, R.C., and Schaber, G.G., 1986, Global radar units on Venus derived from statistical analysis of Pioneer Venus Orbiter radar data: Journal of Geophysical Research, v. 91, no. B5, p. 4979-4992.
Ford, P.G., and Senske, D.A., 1990, The radar scattering properties of Venus landforms: Geophysical Research Letters, v. 17, p.
Head, J.W., Peterfreund, A.R., Garvin, J.B., and Zisk, S.W., 1985, Surface characteristics of Venus derived from Pioneer Venus altimetry roughness and reflectivity measurements: Journal of Geophysical Research, v. 90, no. B8, p. 6873-6885.
Masursky, Harold, Eliason, Eric, Ford, P.G., McGill, G.E., Pettengill, G.H., Schaber, G.G., and Schubert, Gerald, 1980, Pioneer Venus radar results: Geology from images and altimetry: Journal of Geophysical Research, v. 85, no. A13, p. 8232-8260.
Pettengill, G.H., Eliason, Eric, Ford, P.G., Loriot, G.B., Masursky, Harold, and McGill, G.E., 1980, Pioneer Venus radar results: Altimetry and surface properties: Journal of Geophysical Research, v. 85, no. A13, p. 8261-8270.
Pettengill, G.H., Ford, P.G., and Chapman, B.D., 1988, Venus: Surface electromagnetic properties: Journal of Geophysical Research, v. 93, p. 14,881-14,892.
Sjogren, W.L., Phillips, R.J., Birkeland, P.W, and Wimberly, R.N., 1980, Gravity anomalies on Venus: Journal of Geophysical Research, v. 85, no. A13, p. 8295-8302.

See also:
"Pioneer Venus Special Issue," Journal of Geophysical Research, 1980, v. 85, no. A13, p. 7573-8337.

Terrestrial and Lunar Radar Remote Sensing and Geologic Applications

Arvidson, R.E. and 9 others, 1992, Characterization of lava flow degradation in the Pisgah and Cima volcanic fields, California, using Landsat thematic mapper and AIRSAR data: Geological Society of America Bulletin, in press.
Avery, T.E., and Berlin, G.L., 1992, Fundamentals of Remote Sensing and Airphoto Interpretation (5th ed.): Macmillan Publishing Co., New York, 472 p.
Blom, R.G., 1988, Effects of variation in look angle and wavelength in radar images of volcanic and aeolian terrains, or now you see it, now you don't: International Journal of Remote Sensing, v. 9, p. 945-965.
Blom, R.G., and Elachi, Charles, 1987, Multifrequency and multipolarization radar scatterometry of sand dunes and comparison with spaceborne and airborne radar images: Journal of Geophysical Research, v. 92, no. B8, p. 7877-7889.
Campbell, B.A., Zisk, S.H., and Mouginis-Mark, P.J., 1989, A quad-pol radar scattering model for use in remote sensing of lava flow morphology: Remote Sensing of Environment, v. 30, p. 227-237.
Daily, M., Elachi, C., Farr, T., and Schaber, G., 1978, Discrimination of geologic units in Death Valley using dual frequency and polarization imaging radar data: Geophysical Research Letters, v. 5, p. 889–892.
Elachi, Charles, 1987, Introduction to the Physics and Techniques of Remote Sensing: Wiley and Sons, New York.
Evans, D.L., 1992, Geologic studies using synthetic aperture radar (SAR) data: Episodes, v. 15, no. 1, p. 21-31.
Evans, J.V., and Hagfors, T., 1964, On the interpretation of radar reflections from the Moon: Icarus, v. 3, pp. 151-160.
Farr, T., 1992, Microtopographic evolution of lava flows at Cima volcanic field, Mohave Desert, California: Journal of Geophysical Research, v. 97, no. B11, p. 15,171-15,179.

Ford, J.P., 1990, Incidence angle and resolution: Potential effects on interpreting Venusian impact craters in Magellan radar images: Proceedings Lunar and Planetary Science Conference, 20th, p. 573-584.

Ford, J.P., Cimino, J.B., and Elachi, Charles, 1983, Space Shuttle Columbia views the world with imaging radar: The SIR-A experiment: JPL Publication 82-95.

Ford, J.P., Cimino, J.B., Holt, Ben, and Rizek, M.R., 1986, Shuttle imaging radar views the earth from Challenger: The SIR-B Experiment: JPL Publication 86-10.

Gaddis, L., Mouginis–Mark, P., Singer, R., and Kaupp, V., 1989, Geologic analyses of Shuttle Imaging Radar (SIR–B) data of Kilauea Volcano, Hawaii: Geological Society of America Bulletin, v. 101, p. 317–332.

Greeley, Ronald, and Martel, Linda, 1988, Radar observations of basaltic lava flows, Craters of the Moon, Idaho: International Journal of Remote Sensing, v. 9, no. 6, p. 1071-1085.

Hagfors, T., 1970, Remote probing of the Moon by infrared and microwave emissions and by radar: Radio Science, v. 5, pp. 189-227.

Jet Propulsion Laboratory, 1992, Papers presented to the International Colloquium on Venus, August 10-12, 1992, Pasadena, Calif., LPI Contribution No. 789, 137p.

Jet Propulsion Laboratory, 1980, Radar geology: An assessment: Report of the radar geology workshop, Snowmass, Colorado (July 16-20, 1979), JPL Publication 80-61, 513 p.

McCauley, J.F., and 7 others, 1982, Subsurface valleys and geoarchaeology of Egypt and Sudan revealed by Shuttle Radar: Science, v. 218, p. 1004-1020.

Macdonald, H.C., Kirk, J.N., Dellwig, L.F., and Lewis, A.J., 1969, The influence of radar look-direction on the detection of selected geological features: *in* Proceedings of the Sixth International Symposium on Remote Sensing of Environment, Ann Arbor, p. 637-650.

McDonough, M., and Martin-Kaye, P.H.A., 1984, Radargeologic interpretation of Seasat imagery of Iceland: International Journal of Remote Sensing, v. 5, no. 2, p. 433-450.

Moore, H.J., Boyce, J.M., Schaber, G.G., and Scott, D.H., 1980, Lunar remote sensing and measurements: U.S. Geological Survey Professional Paper 1046-B, 78p.

Moore, H.J., and Thompson, T.W., 1991, A radar-echo model for Mars: Proceedings Lunar and Planetary Science Conference, v. 21, p. 457-472.

Sabins, F.F., Jr., 1983, Geologic interpretation of space shuttle radar images of Indonesia: American Association of Petroleum Geologists Bulletin, v. 67, p. 2076-2099.

Sabins, F.F., Jr., 1987, Remote Sensing—Principals and Interpretation (2nd ed.): W.H. Freeman and Co., New York, ch. 6, p. 177-233.

Schaber, G.G., Elachi, Charles, and Farr, T.G., 1980, Remote sensing of SP Mountain and SP lava flow in north-central Arizona: Remote Sensing of Environment, v. 9, p. 149-170.

Schaber, G.G., McCauley, J.F., Breed, C.S., and Olhoeft, G.R., 1986, Shuttle imaging radar: Physical controls on signal penetration and scattering in the Eastern Sahara: IEEE Transactions on Geoscience and Remote Sensing., v. GE-24, no. 4, p. 603-623.

Schaber, G.G., Berlin, G.L., and Brown, W.E., Jr., 1976, Variations in surface roughness within Death Valley, California: Geologic evaluation of 25-cm-wavelength radar images: Geological Society of Americal Bulletin, v. 87, p. 29-41.

Siegal, B.S., and Gillespie, A.R., 1980, Remote Sensing in Geology: Wiley, N.ew York, 702 p.

Thompson, T.W., Masursky, H., Shorthill, R.W., Tyler, G.L., and Zisk, S.H., 1974, A comparison of infrared, radar, and geologic mapping of lunar craters: Moon, v. 10, p. 87-117.

Tyler, G.H., Simpson, R.A., and Moore, H.J., 1971, Lunar slope distributions: Comparisons of bistatic-radar and photogeologic results: Journal of Geophysical Research, v. 76, p. 2790-2795.

Ulaby, F.T., Moore, R.K., and Fung, A.K., 1981, Microwave Remote Sensing—Active and Passive, v. I: Addison-Wesley, Reading, Mass.

Ulaby, F.T., Moore, R.K, and Fung, A.K., 1982, Radar remote sensing and surface scattering and emission theory: *in* Microwave Remote Sensing: Active and Passive, v. II: Addison–Wesley, Reading, Mass., p. 816–880.

Ulaby, F.T., Moore, R.K., and Fung, A.K., 1986, Microwave Remote Sensing—Active and Passive, v. III: Addison-Wesley, Reading, Mass., p. 1935-1999.

Valenzuela, G.R., 1967, Depolarization of EM waves by slightly rough surfaces: IEEE Transactions on Antennas and Propagation, AP–15, p. 552–557.

Van Zyl, J., Burnette, C.F., and Farr, T.G., 1991, Inference of surface power spectra from inversion of multifrequency polarimetric radar data: Geophysical Research Letters, v. 18, no. 9, p. 1787-1790.

APPENDIX A: VMAP PROGRAM PERSONNEL

VMAP Steering Group
(addresses on cover)

Ellen R. Stofan (Chairperson)
Office: (818) 393-0868 or 354-2076
Fax: (818) 393-0530
E-mail: estofan@nasamail.nasa.gov

Philip A. Davis (Vice Chairperson)
Office: (602) 556-7201
Fax: (602) 556-7014
E-mail: pdavis@astrog.span.nasa.gov

Donald B. Campbell
Office: (607) 255-9580
Fax: (607) 255-8803
E-mail: campbell@astrosun.tn.cornell.edu

John E. Guest
Office: 44-81-959-0421
Fax: 44-81-959-0421 (UK office hours only)
E-mail: jeg@starlink.ucl.ac.uk

George E. McGill
Office: (413) 545-0140 or 545-2286
Fax: (413) 545-1200
E-mail: gmcgill@wawa.geo.umass.edu

Patricia G. Rogers (see below)

R. Steven Saunders
Office: (818) 393-0870 or 354-2076
Fax: (818) 393-0530
E-mail: ssaunders@nasamail.nasa.gov

Kenneth L. Tanaka (see below)

James R. Zimbelman
Office: (202) 357-1424
Fax: (202) 786-2566
E-mail: jrz@ceps.nasm.edu

USGS

Map Coordinator
Kenneth L. Tanaka
Office: (602) 556–7208
Fax: (602) 556–7014
E-mail: ktanaka@astrog.span.nasa.gov

Map Editor
Derrick Hirsch
Office: (602) 556–7000
Fax: (602) 556–7014

Cartographic Products
Randolph L. Kirk
Office: (602) 556–7034
Fax: (602) 556–7090
E-mail: rkirk@astrog.span.nasa.gov

IAU Nomenclature Representative
Joel Russell
Office: (602) 556–7211
Fax: (602) 556–7090
E-mail: jrussell@astrog.span.nasa.gov

Mailing address: U.S. Geological Survey
2255 N. Gemini Dr.
Flagstaff, AZ 86001

NASA

Discipline Scientist
Jeffrey Plescia
Office: (202) 358–0292
Fax: (202) 358–3097

Staff Scientist
Patricia G. Rogers
Office: (202) 358–0292
Fax: (202) 358–3097
E-mail: trish@usra.edu

Mailing address:
NASA Headquarters
Code SL
300 E Street, S.W.
Washington, DC 20546

APPENDIX B: SAMPLES OF GEOLOGIC MAP SYMBOLS

[*Notes in brackets*]

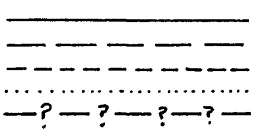

Contact—Long dashed where approximately located; short dashed where indefinite, gradational, or inferred; dotted where concealed; queried where doubtful

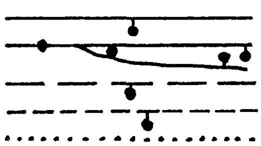

Fault or graben—Long dashed where approximately located; short dashed where inferred or probable; dotted where concealed [must be concealed by overlying mapped deposits]; bar and ball on downthrown side

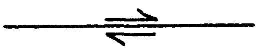

Fault—Arrows show relative horizontal movement

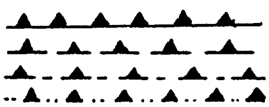

Thrust fault—Sawteeth on upper plate; dashed where approximately located; intermittent dashed where inferred; dotted where concealed

Fault or lineament—Origin uncertain

Tectonic lineament [Used on small-scale tectonic maps]

Joint [Assumed to be vertical]

Ridge crest

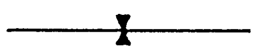

Trough

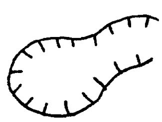

Depression [Includes large volcanic craters]

Scarp—Barb points downslope, line at base

Flow scarp—Hachures on downslope side

Channel

Crater rim crest—Dotted where buried

Small shield [Less than 20 km across]

Large shield [More than 20 km across]

APPENDIX C: RULES AND CONVENTIONS FOR NAMING VENUSIAN FEATURES

The International Astronomical Union (IAU), through its Working Group for Planetary System Nomenclature (WGPSN), is the body that approves names proposed for planetary features. The IAU also makes rules and sets policy regarding planetary nomenclature. The United States is an adherent to the IAU, and we are therefore compelled to follow its dictates in naming planetary features.

Among those rules that apply to Venus are the general rules that persons for whom features are to be named must be well known and deceased for at least three years. Names of persons prominent in any living religion or political or military figures of the 19th and 20th Centuries are disallowed. Furthermore, persons of a specific national significance are not acceptable. These rules are designed to avoid disruptive controversy that could obstruct the naming process.

In addition, the IAU makes rules regarding the kind of names that will be given to different types of features (a list of the feature types approved for Venus that can be named is provided in Table C1). On Venus, craters and volcanic calderas (paterae) are named for women of history; craters less than 20 km in diameter are given female first names from various world cultures. Other types of features are named for mythological women (Table C2). Names proposed for Venusian features must be selected from the proper category; otherwise, they are likely to be rejected. Consideration must also be given to keeping the nomenclature international in scope; that is, we must try to find and apply names from as many nationalities as possible.

Name proposals should be submitted to the USGS in Flagstaff, as the Branch of Astrogeology has been charged by the IAU with the responsibility of maintaining a record of all planetary name requests, as well as managing, updating, and distributing data from the nomenclature master files. Once a specific name has been proposed for a feature, it must be reviewed by two different committees of the IAU. The proposal is then voted upon by the WGPSN at their annual meeting. Once a name has been approved by the WGPSN, it is considered to have "provisional" status. Provisional names may be used in publication, but their provisonal status must somehow be indicated in the publication. (Provisional names on USGS maps are indicated by an asterisk.) The General Assembly of the IAU, which meets triannually, gives final approval to feature names.

Because the naming process is a lengthy one, it behooves mappers to make requests for feature names at the earliest possible time. As base maps become available, ozalid copies will be sent to Venus geologic mappers. Investigators will be asked to identify any unnamed features that they would like to have named. Mappers may propose names themselves, or a feature may be named by the nomenclature representative at USGS (see Appendix A).

Table C1. Feature types approved for use on Venus

FEATURE(S)	DESCRIPTION
Chasma, Chasmata	Canyon
Colles[1]	Small hills or knobs
Corona, Coronae	Ovoid–shaped feature
Crater, Craters	Bowl–shaped depression; impact crater
Dorsum, Dorsa	Ridge
Fluctus, Fluctūs	Flow terrain
Fossa, Fossae	Long, narrow, shallow depression
Linea, Lineae	Elongate marking
Mons, Montes	Mountain
Patera, Paterae	Shallow crater; scalloped, complex edge
Planitia, Planitiae	Low plain
Planum, Plana	Plateau or high plain
Regio, Regiones	Region
Rupes, Rupēs	Scarp
Terra, Terrae	Extensive land mass
Tessera, Tesserae	Tile; polygonal ground
Tholus, Tholi	Small domical mountain or hill
Vallis, Valles	Valley

[1]Used only in plural

Table C2. Categories for naming features on Venus

Feature	Source of name
Chasmata	Goddesses of hunt; Moon goddesses
Colles	Miscellaneous goddesses
Coronae	Fertility goddesses
Craters	Famous women; <20 km, female first names
Dorsa	Sky goddesses
Fluctūs	Goddess, miscellaneous
Fossae	Goddesses of war
Lineae	Goddesses of war
Montes	Goddesses, miscellaneous
Paterae	Famous women
Planitiae	Mythological heroines
Planum	Goddesses of prosperity
Regiones	Giantesses, Titanesses
Rupēs	Goddesses of hearth and home
Tesserae	Goddesses of fate or fortune
Terrae	Goddesses of love
Valles	Word for Venus in various world languages

APPENDIX D: FORMAT INSTRUCTIONS FOR TEXT AND EXPLANATIONS

Headings and Head Notes

Within the description of map units and text, headings are divided into orders—major headings (**INTRODUCTION, PHYSIOGRAPHIC SETTING, STRATIGRAPHY, STRUCTURAL HISTORY, REFERENCES CITED, DESCRIPTION OF MAP UNITS, etc.**) are first–order centered headings and further subdivisions are second order and third order.

Type, centered:

FIRST–ORDER HEADINGS ALL CAPS AND BOLD
SECOND–ORDER HEADINGS ALL CAPS BUT NOT BOLD
Third–order headings initial cap and lowercase and not bold

[Headnotes under centered headings are enclosed in square brackets, extend across entire column width (except centered if only one or two lines long), are not indented, and have no final period]

Map Units and Symbols in DOMU

Type all map unit names at first mention in lowercase and bold; follow by two hyphens. Begin the descriptive material with a capital letter. Do not put a period at the end of the last line of the description of each unit and do not divide the description into paragraphs. Start the name of each first–rank map unit about ten spaces to the right of the first letter of the map unit symbol.

First rank—"Left margin"
  Second rank—Indent two spaces
    Third rank—Indent four spaces
        Fourth rank—Indent eight spaces

All overruns of all ranks—Indent six spaces if more than two ranks are used, four spaces for two ranks, and two spaces for one rank.

Use the same format for symbols (such as contact, fault, etc.) as for map units. On a geologic map, such symbols are explained following the description of map units and a break of about four blank lines but no separate heading.

Example of map explanation. The sample explanation on the following pages demonstrates the application of the above rules (text modified from a Mars map being prepared by S.L. Rotto and K.L. Tanaka). It is made much narrower than an actual explanation to allow room for marginal notes. Note that it is followed by a corresponding correlation chart.

NOTE: This sample is for example purposes only; much of it is out of context.

Headnote
- Square brackets
- If three or more lines, run across entire column width, including symbols
- Centered if only one or two lines
- No final period

First-order centered heading
- All caps
- Bold
- Center over entire column width, including symbols

DESCRIPTION OF MAP UNITS

[Map units distinguished and interpreted on basis of morphology, texture, albedo, and stratigraphic position. Although most map units are rock materials, some channel floors are also considered units in order to highlight erosional events that formed them]

Place here your most significant information that applies to all units

Use telegraphic style! (Incomplete sentences o.k.)

LOWLAND TERRAIN MATERIALS

Chryse assemblage

Basin materials--Form lowland plains below mouths of outflow channels; interpreted to consist of sediments derived from outflow channels and possibly volcanic and eolian deposits. Contacts between basin units generally gradational

First-rank unit
- Caps and lowercase
- Bold
- No indent of first line

Interpretation and other general statements here may obviate need for adding them to subunits below (if they apply to all subunits)

Second-rank unit
- Caps and lowercase
- Bold
- 2-space indent of first line

No final period

cr **Subdued ridged unit**--Plains marked by subdued wrinkle ridges and cut by small outflow channels. *Interpretation:* Ridged plains material partly resurfaced by outflow erosion and deposition

Overruns indented 6 spaces for all ranks

Left margin at least 1"

Right margin at least 1"
Do not justify

Allow about 10 spaces; some letter symbols may be as long as 5 spaces

cc **Complex unit**--Characterized by one or more of the following: (1) hummocky topography; (2) small knobs (some superposed on mesas); (3) sinuous depressions about 10 km wide and tens of kilometers long; (4) sinuous ridges less than 1 km wide, some of which are medial in sinuous depressions or connect knobs; (5) narrow, curvilinear, northeast-trending grooves; and (6) several mostly buried crater rims. Unit gradational with smooth and grooved basin materials. *Interpretation:* Relatively thick lacustrine deposits from most recent flooding. Various features result of fluvial or glacial processes (or both) and compaction of sediments

Write out "kilometers" where not preceded by numerals

Note clear separation of observations and interpretation

Use this wording instead of "and/or" (which USGS doesn't permit)

cu **Undivided unit**--Material of Chryse assemblage occurring where image resolution does not permit discrimination of individual units

Text • Closed up to hyphens • Following hyphens -begins with cap letter -not bold			
First-rank unit		**Knobby materials**--Interpreted as basin sediments and perhaps lava flows that embay knobs of older degraded plateau material	
Second-rank unit	ck	**Younger knobby material**--Forms knobby plains. Cut by lowermost Ares Vallis; gradational with older knobby material; embays mouth of Mawrth Vallis	
Third-rank units • Caps and lowercase • Bold • 4-space indentation of first line	cku	**Upper unit**--Found only in upper reaches of Kasei Valles in southwest quadrant of map area	
	ckl	**Lower unit**--Locally underlies upper unit but most exposures found in lower reaches of Kasei Valles in north-central part of map area	Describe relations of units after last (oldest) unit is identified
Use "type area" only when formally proposing geol. name (note also style of map coordinates)	cko	**Older knobby material**--Closely spaced groups of knobs on high, undulatory plains along highland-lowland boundary (fig. 1). Typical exposures at lat 14.4°N., long 172° (Viking frame 639A12)	All geographic features mentioned should be located (1) on main map, (2) in a figure that is referenced here, or (3) in words earlier in text

HIGHLAND TERRAIN MATERIALS

Tharsis assemblage

[Lava flows originating in Tharsis region]

Tharsis Montes Formation--Easternmost flows of large shields of Tharsis Montes; exposed in western part of map area

Capital "F" in "Formation" because it is formal geol. name

Give locations of outcrop areas if too small for reader to locate quickly (note use of "map area," not "map")

t5 **Member 5**--Marked by elongate, high-albedo flow lobes with distinct margins; craters rare. Correlative with member 3 of Tharsis Montes Formation as mapped by Doakes (1983)

Avoid use of "with" where possible. Here, substitute "having"

This is most visible location for information on correlation

Lowercase "m" in "member" because it is informal geol. name (Note that "member 3" is written out, not referred to by symbol t3)

NOTE: In explanation of map symbols, overruns have same indentation as overruns in Description of Map Units (6 spaces in this example).

Sample Correlation Chart

The following correlation chart corresponds to the above description of map units:

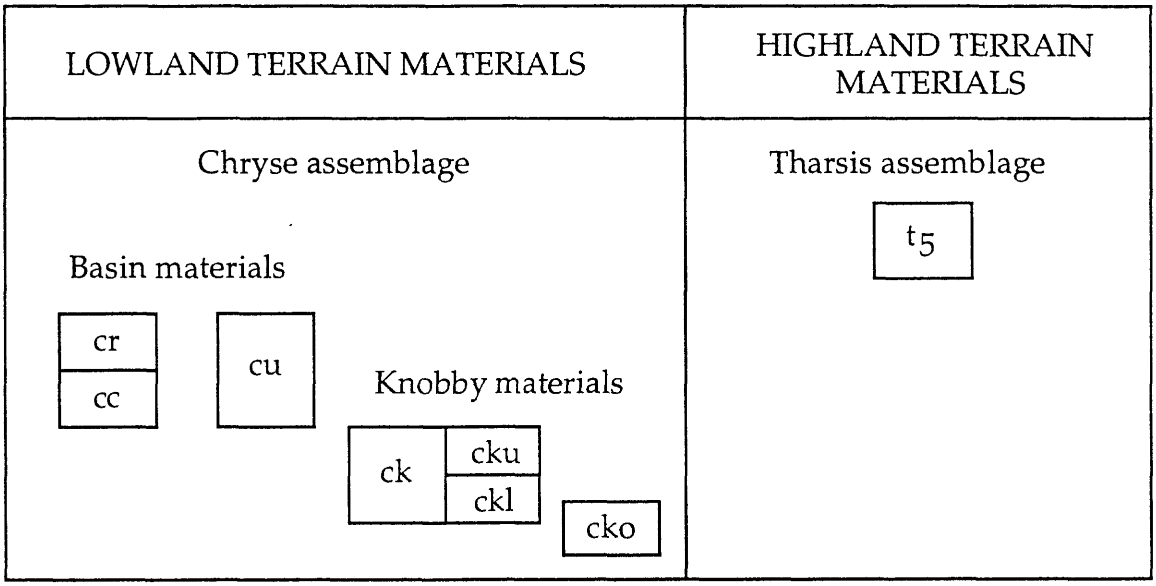

APPENDIX E

Submission Checklist For Planetary Geologic Maps

Map Title:____

Author(s):____

Submission date:____________________________________

Date of completion of coordinator review:________________________

(A) Geologic Map (and Cross Sections)

______ (1) All outcrops are labeled with unit symbols; symbols and colors are same as those elsewhere in material.

______ (2) Contact lines are complete and neat. Check for line breaks and irregularities.

______ (3) Dashed, buried, and queried lines and scratch contacts, if used, are clearly shown. (For economy's sake avoid dashing long stretches; instead explain in text the indefinite nature of contact.)

______ (4) Superposition relations are clear and consistent with text.

______ (5) Line symbols match those of earlier adjoining maps where possible; if not, discrepancies are explained in text.

______ (6) Structural symbols are clearly identified and have obviously thicker line weight than contacts.

______ (7) Cross sections are consistent with map in every detail. (See Suggestions to Authors.)

(B) Description of Map Units (DOMU) and Explanation

______ (1) Format of DOMU follows conventions shown in Appendix D, Venus Geologic Mappers' Handbook (give close attention to this!)

______ (2) Order of DOMU follows order of correlation chart. Map units described by grouping in chart (from left to right) and then from youngest to oldest (see DOMU and chart samples. Appendix D, VGM Handbook).

______ (3) Each map unit is described in following order: (1) Definitive characteristics, (2) secondary characteristics, (3) stratigraphic information, (4) location (if not obvious on map), (5) type area (optional; for new units only), and (6) interpretation (separate from description.

______ (4) All unit and feature symbols on map are shown and explained (and vice versa); symbols follow precedents where applicable.

(C) Correlation Chart

______ (1) A box for each map unit is included and properly colored.

______ (2) All unit groups and subgroups are shown, as well as their names. (See example of correlation chart in Appendix D, VGM Handbook)

______ (3) All stratigraphic positions are shown by relative vertical ranges of unit boxes and match relations and descriptions shown on map and in text and DOMU. Major stratigraphic divisions (e.g., Amazonian, Hesperian, and Noachian) and crater-density correlations are shown where applicable.

(D) Map Text

______ (1) Text is in logical order (e.g., Introduction, Stratigraphy, Structure (and(or) other special sections), and summary).
______ (2) Under Introduction, note briefly any previous work in area, its scale, and type of images on which it was based; also, note resolution(s) of images used in present mapping.
______ (3) Under Stratigraphy, units and events are described from oldest to youngest.

______ (4) Geographic names mentioned are shown on map base or in a figure, or their map coordinates are given in text. (In preparation of published map, drafters will routinely transfer to it all nomenclature from base.)
______ (5) Unit names agree exactly with terms used in DOMU (do not paraphrase).

______ (6) All references are listed in "References cited."

(E) References Cited

______ (1) All references cited appear elsewhere in the copy material.

______ (2) USGS reference format style is followed (See USGS Suggestions to Authors or reference list on p. 30-32 in VGM Handbook.)

(F) Additional Figures, Tables and Color Plates (if any)

______ (1) Figures and tables in text are numbered sequentially.

______ (2) Each figure and table should stand alone. (Caption contains all information necessary for comprehension, and text does not repeat this information.)
______ (3) For images, north and illumination directions and image number(s) are noted; scale bar is provided. Use annotations showing discussed features.

(G) Enclosed Materials
(Keep brownline and originals of images until they are requested)

______ (1) One colored and three uncolored copies of map, correlation chart, and any color plates or cross sections.
______ (2) Three copies of map text, DOMU, explanation, figures and captions, and tables.

______ (3) Include any special instructions in cover letter.

______ (4) Completed check list.

Send materials to:

Ken Tanaka
PGM Coordinator
USGS
2255 N. Gemini Dr.
Flagstaff, AZ 86001

If you need assistance in using this checklist, please call Ken Tanaka at (602) 556-7208; FAX (602) 556-7014; E-MAIL ktanaka@astrog.span.nasa.gov

APPENDIX F

Technical Reviewer's Checklist for Planetary Geologic Maps

Map Title:____

Author(s):____

Reviewer:____

Date sent to reviewer:____________Date returned to USGS map coordinator:______________

(A) Geologic map

_____ **If checked here, color each unit of uncolored map ozalid.**

Check for the following:

_____ (1) Completeness of contacts

_____ (2) Correctness of map-unit symbols (compare with DOMU)

_____ (3) Consistency of line symbols (dashed where gradational or approximate, dotted where buried, or queried where uncertain). Structure symbols have thicker lines than contacts

_____ (4) Agreement of triple junctions of contacts with stratigraphy shown in correlation chart

_____ (5) Correct coloring of author-supplied copy

_____ (6) Consistency of detail throughout map (unless image resolution changes dramatically); map neither overly cluttered with symbols and unnecessary line work nor overgeneralized. (If more detail is required in an especially complex area, an inset map at larger scale may be included.)

_____ (7) Geographic nomenclature is correctly shown and adequate

_____ (8) Reasonable match of borders with borders of previously submitted maps at same scale (contacts, structure, relative ages). If author of later map cannot match, he/she should explain in DOMU.

(B) Description of map units (DOMU)

_____ (1) Unit names and symbols follow precedents, where applicable

_____ (2) Units are mappable based on described characteristics

_____ (3) Important stratigraphic relations are noted

_____ (4) Location noted if occurrence restricted

_____ (5) Interpretation clearly separated from description; description contains no genetic terms; interpretation(s) consistent with unit description

_____ (6) If type area is noted, it is the most definitive exposure

_____ (7) Unit groupings have precedent or are clearly defined

______ (8) Format follows USGS guidelines (see VGM Handbook, Appendix D)

(C) Correlation chart

______ (1) Relative ages of units agree with stratigraphic information in DOMU and crater-count data (if applicable)

______ (2) Format follows USGS guidelines (see VGM Handbook, Appendix D)

(D) Explanation of map symbols

______ (1) Symbols are clearly defined, distinct, and agree with precedents where applicable

(E) Map text

______ (1) Discussions are based mainly on map data; all appropriate references are cited (involved analyses should be presented in a journal article)

______ (2) Good balance in presentation of interpretations (not overly biased or extensive)

______ (3) Previous work referenced; significant departures in mapping from same data are discussed

______ (4) Text agrees with other components of map; not overly redundant with DOMU

______ (5) Introductory material is useful. It generally includes brief discussions of the geologic and physiographic settings, data sources, and previous work

______ (6) Where geology is complex, special sections and (or) summary are provided

______ (7) Location of each feature refrred to is clear on map or a figure or is given verbally in text

(F) Cross sections (if applicable)

______ (1) Topographic profile drawn accurately on stable material (such as mylar)

______ (2) Consistent with stratigraphy and structure shown on map and correlation chart and described in text

______ (3) Line(s) of section and vertical exaggeration (if any) chosen to best show the structure

(G) Figures and tables

______ (1) New, map-based numerical data presented in tables and (or) graphs (e.g., crater counts, remote-sensing data for map units)

In addition to completing this checklist, please annotate map materials with your comments. Lengthier comments should be typed separately. Please return all materials originally received (including route sheet signed by reviewer or initialed if reviewer requires a second look at the map) for the review to:

Ken Tanaka
PGM Coordinator
USGS
2255 N. Gemini Dr.
Flagstaff, AZ 86001

If you need assistance in using this checklist, please call Ken Tanaka at (602) 556-7208; FAX (602) 556-7014; E-MAIL ktanaka@astrog.span.nasa.gov